NASA Technical Memorandum 89102

High Reynolds Number Tests of the NASA SC(2)-0012 Airfoil in the Langley 0.3-Meter Transonic Cryogenic Tunnel

Raymond E. Mineck and Pierce L. Lawing

JULY 1987

NASA

NASA Technical Memorandum 89102

High Reynolds Number Tests of the NASA SC(2)-0012 Airfoil in the Langley 0.3-Meter Transonic Cryogenic Tunnel

Raymond E. Mineck and Pierce L. Lawing
Langley Research Center
Hampton, Virginia

National Aeronautics
and Space Administration

**Scientific and Technical
Information Office**

1987

SUMMARY

A wind-tunnel investigation of the NASA SC(2)-0012 airfoil has been conducted in the Langley 0.3-Meter Transonic Cryogenic Tunnel. This supercritical airfoil section is 12 percent thick and symmetrical. This investigation supplements the two-dimensional airfoil studies of the Advanced Technology Airfoil Test program. Tests were conducted at various combinations of stagnation temperature and pressure to cover a Mach number range from 0.60 to 0.84 and a Reynolds number range from 6 to 40×10^6 based on a 6.0-in. (15.24-cm) airfoil chord. The angle of attack was varied from -4.0° to 4.5°.

No corrections for wind-tunnel wall interference have been made to the data. The aerodynamic results are presented as pressure distributions and integrated force and moment coefficients without any analysis.

INTRODUCTION

The National Aeronautics and Space Administration (NASA) has conducted a systematic study of well-known conventional airfoils and advanced technology airfoils over a wide range of Reynolds number. This study, described in detail in reference 1 and referred to as the Advanced Technology Airfoil Tests (ATAT) program, was carried out in the Langley 0.3-Meter Transonic Cryogenic Tunnel (0.3-m TCT). The program was divided into two phases: a correlation phase involving conventional and advanced airfoils tested in other facilities and an advanced technology phase involving new airfoils without a significant data base. One of the objectives of the program was to expand the airfoil data base at high Reynolds numbers.

One of the airfoils tested in the correlation phase of the ATAT program was part of a family of supercritical airfoils developed by NASA. Details of the design philosophy used to develop the family of airfoils are presented in reference 2. This airfoil was designed for application to a transport-type airplane wing, and the results are presented in reference 3. The family also included a symmetric supercritical airfoil for nonlifting applications such as the vertical tail on a transport-type airplane. A model of this airfoil was built to demonstrate a novel model fabrication technique described in reference 4. This model was tested in the 0.3-m TCT to determine if there were any limitations associated with the fabrication technique when the model was subjected to load at cryogenic temperatures. The results would add high Reynolds number data for a symmetric supercritical airfoil to the ATAT airfoil data base of cambered supercritical airfoils.

The model tests of the symmetric supercritical airfoil were conducted in the 8-in. by 24-in. (20-cm by 60-cm) two-dimensional test section of the 0.3-m TCT. Reference 5 describes the operating characteristics and operating envelope of the tunnel. Tests were conducted at various combinations of stagnation temperature and pressure to cover a Mach number range from 0.60 to 0.84 and a Reynolds number range from 6 to 40×10^6 based on the airfoil chord. Integrated forces and moments and a summary of the airfoil chordwise pressure distributions are presented at selected values of Mach number and Reynolds number without analysis.

SYMBOLS

The measurements and calculations were made in U.S. Customary Units. These measurements have been converted to the International System of Units (SI) which are shown in parentheses. Factors relating the two systems of units are presented in reference 6.

b	model span, 8.0 in. (20.32 cm)
C_d	section drag coefficient measured on tunnel centerline, positive downstream
C_m	section pitching moment, resolved about quarter-chord point, positive nose up
C_n	section normal-force coefficient, positive in z-direction
C_p	local pressure coefficient
c	model chord, 6.0 in. (15.24 cm)
M_∞	free-stream Mach number
R_c	free-stream Reynolds number based on model chord
x	chordwise position from leading edge of model (positive aft), in. (cm)
y	spanwise position on model from centerline (positive to right looking upstream), in. (cm)
z	vertical distance from model chord plane (positive measured up), in. (cm)
α	section geometric angle of attack (positive leading edge up), deg
σ_M	standard deviation in Mach number during a data recording
σ_R	standard deviation in Reynolds number during a data recording

WIND TUNNEL AND MODEL

Wind Tunnel

The tests were conducted in the 8-in. by 24-in. (20-cm by 60-cm) two-dimensional, slotted-wall test section of the 0.3-m TCT. A schematic diagram of the tunnel showing the various components is presented in figure 1. A photograph of the tunnel is presented in figure 2. The 0.3-m TCT is a continuous-operation, fan-driven, cryogenic pressure tunnel that uses gaseous nitrogen as a test medium. The tunnel is capable of operating at stagnation temperatures from just above the boiling point of liquid nitrogen (LN_2), approximately 80 K, to just above room temperature, approximately 327 K, and at stagnation pressures from 1.2 to 6.0 atm. The test-section Mach number has been calibrated from 0.20 to about 0.92. This combination of test conditions provides Reynolds numbers up to 55×10^6 based on a model chord of 6.0 in. (15.24 cm). Additional details about the tunnel may be found in reference 5.

A photograph of a model in the test section is presented in figure 3. The top of the plenum and the test-section top wall (ceiling) have been removed to show the model installation. The two-dimensional test section has solid sidewalls and a slotted top wall (ceiling) and bottom wall (floor). There are two slots in the top and bottom slotted walls with pressure orifices located on the centerline on the slat between the slots. A photograph of the model mounted between the turntables just prior to installation in the test section is presented in figure 4, and a sketch of the test section is presented in figure 5.

A computer-driven mechanism controls the angular position of the turntables to set the angle of attack (AOA). The mechanism has a traversing range from -20° to 20°, which can be offset from 0° in either direction during the model installation. It is driven by an electric stepper motor, which is connected through a yoke to the perimeter of both turntables. This arrangement drives both ends of the model through the angle-of-attack range to eliminate possible model twisting. The angular position of the turntables and, therefore, the geometric angle of attack of the model are recorded using the output of a digital shaft encoder that is geared to one of the turntables.

A computer-controlled survey mechanism traverses a momentum rake vertically to measure the total pressure loss in the model wake. The mechanism provides two mounting locations on the left sidewall for the rake: either at tunnel station 8.3 in. (21.0 cm) or at 10.2 in. (26.0 cm). For this test, the wake survey measurements were made at the rear station, which placed the measurement plane about 1.2 chord lengths downstream of the airfoil trailing edge. The survey mechanism is driven by an electric stepper motor and is designed to translate the rake at speeds from about 0.1 in/sec (0.25 cm/sec) to about 6 in/sec (15 cm/sec). It has a total traversing range of 10 in. (25.4 cm). The stroke (that portion of the total traversing range used in a given survey), the number of points in a survey, the number of samples at each point in the survey, and the speed of the survey mechanism can be controlled by the operator in the control room to meet the research requirements. The vertical position of the rake is recorded using the output from a digital shaft encoder geared to the survey mechanism.

The momentum rake has nine total pressure probes as shown in figure 6. The six active probes used in this test were located at the following spanwise stations: $y/(b/2) = 0$ (centerline), -0.125, -0.250, -0.375, -0.500, and -0.750.

Model

The model used in this test was a 12-percent-thick, symmetric, advanced technology supercritical airfoil designed by NASA for a Reynolds number of 30×10^6. The model chord is 6.0 in. (15.24 cm). The design and measured model ordinates are presented in table I. It should be noted that the airfoil design technique was applied up to the 60-percent-chord station. The rest of the airfoil was defined as a straight line to the trailing edge. The model was fabricated using a novel process described below; details are available in reference 4.

The model was designed as two mating halves with channels routed into the mating surfaces to provide a path between tubing leading to the pressure measurement system and the pressure orifice. A photograph of the model at this stage in the fabrication is shown in figure 7. At one end of the channel, the pressure orifices are predrilled outward from the mating surface at the proper angle to intersect the model surface after the final machining. At the opposite end, tubes are brazed in to form

a connection with the wind-tunnel pressure instrumentation system. The photograph also shows the channels matching on both surfaces to form pressure orifices at the trailing edge. The fan-shaped channel configurations are the top and bottom leading-edge pressure orifice rows.

After the machining on the mating surfaces is complete, the two halves of the model are assembled with brazing foil between the mating surfaces and with the connector tubes in place. The model is then placed in a vacuum-brazing oven. Weights are placed on the model to provide a moderate pressure to force the two pieces together as the brazing foil melts. The model can then be rough machined and the integrity of the pressure orifices verified before the final machining is done.

This fabrication process provided much freedom in selecting the location of the pressure orifices. The orifices were arranged as shown in figure 8. This report presents the results from the chordwise rows staggered near the centerline on the upper and lower surfaces. There were 25 orifices on the upper surface and 27 on the lower surface. All pressure orifices were 0.010 in. (0.25 mm) in diameter except for the short chordwise row of orifices to the right of the centerline which were 0.005 in. (0.13 mm) in diameter. A listing of the orifice locations is presented in table II.

TEST INSTRUMENTATION AND PROCEDURES

Test Instrumentation

A detailed discussion of the instrumentation and procedures for the calibration and control of the 0.3-m TCT can be found in reference 7. For two-dimensional airfoil tests, the 0.3-m TCT is equipped to obtain static pressure measurements on the airfoil model surface, total pressure measurements in the model wake, and static pressure measurements on the sidewalls, top wall, and bottom wall of the test section. Except for the wall pressures, all measurements use individual pressure transducers.

Tunnel test conditions.- The tunnel test conditions were determined by three primary measurements: the total pressure, the static pressure, and the total temperature. The total pressure and static pressure were measured by individual quartz differential pressure transducers referenced to a vacuum. The transducer has a range from -100 to +100 psid (-6.8 to +6.8 atm). It has an accuracy of ±0.006 psid (±0.0004 atm) plus ±0.012 percent of the pressure reading. The stagnation temperature was measured by a platinum resistance thermometer. The analog output from these devices was converted by individual digital voltmeters. Further details of this instrumentation are presented in reference 7.

Airfoil model pressures.- The pressures on the airfoil model are measured by individual transducers connected by tubing to each orifice on the model. The transducers are of a commercially available, high-precision, variable-capacitance type. The maximum range of these differential transducers is from -100 to +100 psid (-6.8 to +6.8 atm) with an accuracy of ±0.25 percent of the reading from -25 to +100 percent of full scale. They are located external to the tunnel and its high-pressure cryogenic environment, but as close as possible to the test section to minimize the tubing length and reduce the response time. To provide increased accuracy, the transducers are mounted both on thermostatically controlled heater bases to maintain a constant temperature and on "shock" mounts to reduce possible vibration effects. The electrical signals from the transducers are connected to individual signal conditioners located in the tunnel control room. The signal conditioners are

autoranging and have seven ranges available. As a result of the autoranging capability, the analog output to the data acquisition system is kept at a high level even though the pressure transducer may be operating at the low end of its range.

Wall pressures.- The tunnel floor and ceiling pressures are measured using a scanivalve system capable of operating ten 48-port scanivalves. Because of the large changes in the pressure of the tunnel over its operational range, the same capacitance-type pressure transducers and autoranging signal conditioners described above are used in the scanivalve instead of the more typical strain gauge transducer. These pressures are normally used in the wall correction procedure and are not presented in this report.

Wake pressures.- The total pressure loss in the model wake is measured with the momentum rake described previously. The pressure in each of the six operational tubes is measured with the same type of pressure transducer described above. The static pressures on the right sidewall at nine vertical positions at the tunnel station opposite the momentum rake are measured with nine individual pressure transducers. The transducers used are of the same capacitance type described above but with a maximum range from -20 to +20 psid (-1.36 to +1.36 atm).

Procedures

Figure 9 shows the test program (R_c versus M_∞) used in this investigation. For these tests, no transition strip was placed on the model because of the high Reynolds number capability of the 0.3-m TCT. The selection of test conditions was made in an effort to overlap experimental and theoretical work for some of the airfoils tested in the ATAT program.

The following procedure was used to set the test conditions. The tunnel total pressure and temperature and the fan speed were set for the desired Mach number and Reynolds number. The angle of attack was set for near-zero model lift and then the data were recorded. The angle of attack was then increased to the next angle, the tunnel conditions were adjusted, and the data were recorded. If the angle exceeded the desired value when setting the angle of attack, the angle was reduced well below the desired angle before attempting to reset the angle again. This is a standard testing technique to minimize the possibility of hysteresis effects. This process was repeated up to the maximum positive angle of 4.5°. The angle of attack was then returned to near-zero model lift and the process was repeated for increasing negative angles of attack.

At the beginning of the data recording process, the computer surveys the model wake and presents the results graphically to the operator. The operator then chooses the stroke (the upper and lower traversing limits) for this data point so that about 80 percent of the points are within the wake. The rake is then positioned to the beginning of the stroke near the ceiling. Twenty samples of the airfoil static pressures, the test conditions, the momentum rake total pressures, the wake static pressures, and the wall pressures on the scanivalve were recorded over a period of 1 sec. Since there were individual transducers for each orifice on the model, each sample consisted of simultaneous static pressure readings from all orifices on the model. These 20 samples were used to compute the test conditions, the normal force, and the pitching moment. The wake survey mechanism was synchronized with the scanivalves so that the rake was moved to the next vertical location when the scanivalves advanced to a new port. After the appropriate settling time, another 20 samples were recorded at the new rake location. This procedure continued until the scanivalves

completed their stepping at which time the rake continued to step at a predetermined rate through the remaining portion of the wake. For this test, the number of steps within the stroke was held constant at 50.

DATA ACQUISITION, REDUCTION, AND QUALITY

Data Acquisition

Data were recorded on magnetic tape with a computer-controlled, high-speed, digital data acquisition system located in the control room of the 0.3-m TCT. This system has a total of 192 analog channels with 8 selectable ranges from ±4 to ±131 mV and a resolution of 1 part in 8191. In addition, there are 16 digital input channels. All analog data were filtered with a 10-Hz low-pass filter. An operating and acquisition program is used by the computer to scan the data acquisition hardware and to write the raw data on tape.

Data Reduction

The test Mach number is based on an average of the Mach number distributions measured on the turntables during the calibration of the "empty" test section. Because the tunnel operating envelope includes high pressures and low temperatures, real-gas effects are included in the data reduction for the tunnel test conditions using the thermodynamic properties of nitrogen gas calculated from the Beattie-Bridgeman equation of state. This equation of state has been shown in reference 8 to give essentially the same thermodynamic properties and flow calculation results in the temperature-pressure regime of the 0.3-m TCT as those given by the more complicated Jacobsen equation of state. Detailed discussions of real-gas effects when testing in cryogenic nitrogen are contained in references 9 and 10.

Section normal-force and pitching-moment coefficients are calculated using the first 20 samples from numerical integration (based on the trapezoidal method) of the local surface pressure coefficient measured at each orifice multiplied by an appropriate weighting factor (incremental area).

The section drag coefficient is calculated from the wake survey pressures by first computing an incremental or point drag coefficient by the method of reference 11 for each rake tube pressure at each rake position. These point drag coefficients are then numerically integrated across the model wake, again based on the trapezoidal method. Specifically, the point drag coefficients are compared one by one to a "threshold" value of drag coefficient which accounts for a nonzero pressure decrement outside the model wake. Based on experience from previous tests, the threshold value was set at 0.0002 for this test. If, in the integrating process, the individual coefficient is greater than or equal to the threshold value, the weighting factor (incremental area) is applied and the incremental drag is included in the running sum of the total drag. If the individual coefficient is less than the threshold, the weighting factor is set equal to zero and the incremental drag is not included in the running sum of the total drag. The results of this integration are total drag coefficients at each of the six momentum rake tube locations. The data reduction program then provides a correction which subtracts that summed portion of the individual incremental drag coefficients within the wake that is attributable to the threshold level. These corrected values are the ones used for the discussion of all the drag data. In this report, all drag data pertain to the tube on the tunnel centerline.

Data Quality

In all wind-tunnel testing, and especially in transonic testing, the steadiness of the tunnel flow conditions, such as Mach number, have direct bearing on the quality of the final aerodynamic data. With the use of individual pressure transducers on each of the model pressure orifices, and with all the model data being recorded at the time of the first rake step, Mach number fluctuations in the surface pressure, normal force, and pitching-moment data for any given point are essentially nonexistent. The possibility of Mach number fluctuations during the time required for the rake to complete the survey of the wake was checked for several angles of attack for a single set of tunnel test conditions, $M_\infty = 0.60$ and 0.80 at $R_C = 6$, 15, and 40×10^6 at zero lift. The standard deviations in Mach number σ_M and in Reynolds number σ_R during the wake surveys are given, respectively, as follows:

M_∞	Standard deviation in Mach number σ_M for Reynolds numbers of -		
	6×10^6	15×10^6	40×10^6
0.60	0.0009	0.0006	0.0011
.80	.0029	.0014	.0014

M_∞	Standard deviation in Reynolds number σ_R for Reynolds numbers of -		
	6×10^6	15×10^6	40×10^6
0.60	0.011	0.012	0.070
.80	.015	.021	.099

The tunnel sidewalls induce an error in Mach number; the slotted top and bottom walls can induce an error in angle of attack and Mach number because of the model lift and blockage. No corrections for wall effects have been applied to the experimental data presented in this report.

PRESENTATION OF RESULTS

The results are presented in the following order:

DISCUSSION

The effect of Mach number on the integrated force and moment coefficients is presented in figure 10. Zero lift did not coincide with 0° angle of attack. The difference may be attributed to a misalignment between the surface used to set 0° angle of attack and the model chord plane, to the difference between the design and measured model ordinates, or to flow angularity.

The effect of chord Reynolds number on the integrated force and moment coefficients is presented in figure 11. There was only a small effect of chord Reynolds number on the model normal-force and pitching-moment results. There was a more significant effect on the drag, especially at the lower chord Reynolds number.

The effect of angle of attack on the chordwise pressure distributions is presented in figures 12 to 16. The plots have been arranged so that corresponding positive and negative normal-force coefficients are side by side. The pressure distributions are consistent; that is, the upper surface pressure distribution at a positive normal force is virtually the same as the lower surface pressure distribution at the same negative normal-force coefficient. The effect of Mach number on the chordwise pressure distribution is presented in figure 17 for near-zero normal-force coefficient.

The model was inspected after testing was completed. No mechanical problems such as debonding of the model halves and warping of the model surface were detected. This inspection, along with the consistent pressure distributions described above, demonstrate that the novel model fabrication technique is acceptable for cryogenic wind-tunnel models.

CONCLUDING REMARKS

A wind-tunnel investigation of the NASA SC(2)-0012 airfoil has been conducted in the Langley 0.3-Meter Transonic Cryogenic Tunnel. This investigation supplements the NASA/U.S. industry two-dimensional airfoil studies of the Advanced Technology Airfoil Test program. This investigation was designed to demonstrate a novel model fabrication technique and to test a NASA advanced technology airfoil from low to flight-equivalent Reynolds numbers.

Both objectives of this investigation were met. The results are presented in graphical form without corrections.

NASA Langley Research Center
Hampton, VA 23665-5225
May 1, 1987

REFERENCES

1. Ladson, Charles L.; and Ray, Edward J.: Status of Advanced Airfoil Tests in the Langley 0.3-Meter Transonic Cryogenic Tunnel. Advanced Aerodynamics - Selected NASA Research, NASA CP-2208, 1981, pp. 37-53.

2. Whitcomb, Richard T.: Review of NASA Supercritical Airfoils. ICAS Paper No. 74-10, Aug. 1974.

3. Harris, Charles D.: Aerodynamic Characteristics of a 14-Percent-Thick NASA Supercritical Airfoil Designed for a Normal-Force Coefficient of 0.7. NASA TM X-72712, 1975.

4. Lawing, Pierce L.: The Construction of Airfoil Pressure Models by the Bonded Plate Method: Achievements, Current Research, Technology Development and Potential Applications. NASA TM-87613, 1985.

5. Ray, Edward J.; Ladson, Charles L.; Adcock, Jerry B.; Lawing, Pierce L.; and Hall, Robert M.: Review of Design and Operational Characteristics of the 0.3-Meter Transonic Cryogenic Tunnel. NASA TM-80123, 1979.

6. Mechtly, E. A.: The International System of Units - Physical Constants and Conversion Factors (Second Revision). NASA SP-7012, 1973.

7. Ladson, Charles L.; and Kilgore, Robert A.: Instrumentation for Calibration and Control of a Continuous-Flow Cryogenic Tunnel. NASA TM-81825, 1980.

8. Hall, Robert M.; and Adcock, Jerry B.: Simulation of Ideal-Gas Flow by Nitrogen and Other Selected Gases at Cryogenic Temperatures. NASA TP-1901, 1981.

9. Adcock, Jerry B.: Real-Gas Effects Associated With One-Dimensional Transonic Flow of Cryogenic Nitrogen. NASA TN D-8274, 1976.

10. Adcock, Jerry B.; and Johnson, Charles B.: A Theoretical Analysis of Simulated Transonic Boundary Layers in Cryogenic-Nitrogen Wind Tunnels. NASA TP-1631, 1980.

11. Baals, Donald D.; and Mourhess, Mary J.: Numerical Evaluation of the Wake-Survey Equations for Subsonic Flow Including the Effect of Energy Addition. NACA WR L-5, 1945. (Formerly NACA ARR L5H27.)

TABLE I.- DESIGN AND MEASURED AIRFOIL ORDINATES

(a) Upper surface

x/c	z/c ordinates for -	
	Design	Measured
0	0	0
.002	.00912	
.005	.01392	
.010	.01860	
.020	.02484	
.030	.02916	.02958
.040	.03240	
.050	.03504	
.060	.03732	.03742
.080	.04119	
.100	.04428	
.120	.04680	
.140	.04908	.04915
.160	.05100	
.180	.05268	.05271
.200	.05412	
.220	.05532	.05529
.240	.05640	
.260	.05736	
.280	.05808	
.300	.05880	.05865
.320	.05928	
.340	.05964	
.360	.05988	
.380	.06000	
.400	.06000	.05986
.420	.05988	
.440	.05964	
.460	.05928	
.480	.05880	
.500	.05808	.05792
.520	.05736	
.540	.05640	
.560	.05520	
.580	.05388	
.600	.05232	
.620	.05040	
.640	.04824	
.660	.04584	
.680	.04332	
.700	.04080	.04052
.720	.03828	
.740	.03576	
.760	.03324	
.780	.03072	
.800	.02820	
.820	.02568	
.840	.02316	.02294
.860	.02064	
.880	.01812	
.900	.01560	
.920	.01308	
.940	.01056	
.960	.00804	
.983	.00510	.00477
1.000	.00300	

(b) Lower surface

x/c	z/c ordinates for -	
	Design	Measured
0	0	0
.002	-.00912	
.005	-.01392	
.010	-.01860	
.020	-.02484	
.030	-.02916	
.040	-.03240	
.050	-.03504	
.060	-.03732	-.03793
.080	-.04119	
.100	-.04428	
.120	-.04680	
.140	-.04908	-.04945
.160	-.05100	
.180	-.05268	
.200	-.05412	
.220	-.05532	-.05570
.240	-.05640	
.260	-.05736	
.280	-.05808	
.300	-.05880	
.320	-.05928	
.340	-.05964	
.360	-.05988	
.380	-.06000	
.400	-.06000	-.06029
.420	-.05988	
.440	-.05964	
.460	-.05928	
.480	-.05880	
.500	-.05808	
.520	-.05736	
.540	-.05640	
.560	-.05520	
.580	-.05388	
.600	-.05232	
.620	-.05040	
.640	-.04824	
.660	-.04584	
.680	-.04332	
.700	-.04080	-.04093
.720	-.03828	
.740	-.03576	
.760	-.03324	
.780	-.03072	
.800	-.02820	
.820	-.02568	
.840	-.02316	-.02338
.860	-.02064	
.880	-.01812	
.900	-.01560	
.920	-.01308	
.940	-.01056	
.960	-.00804	
.980	-.00552	
1.000	-.00300	

TABLE II.- PRESSURE ORIFICE LOCATIONS

(a) Upper surface chordwise row locations

Orifice	x/c	$\frac{y}{b/2}$	z/c
1	0	-0.1000	0
3	.0020	-.1500	.0091
4	.0040	-.1750	.0125
7	.0250	-.2500	.0271
8	.0400	-.2750	.0324
10	.1000	-.0600	.0443
11	.1400	-.0437	.0491
13	.2200	-.0838	.0553
14	.2600	-.0677	.0574
15	.3000	-.0518	.0588
17	.3800	-.1000	.0600
18	.4200	-.0838	.0599
19	.4600	-.0677	.0593
20	.4800	-.0597	.0588
21	.5000	-.0518	.0581
22	.5200	-.0437	.0574
23	.5400	-.0355	.0564
26	.6000	-.0838	.0523
27	.6400	-.0677	.0482
28	.6800	-.0518	.0433
29	.7200	-.0355	.0383
30	.7600	-.0195	.0332
31	.8000	-.1000	.0282
32	.8400	-.0838	.0232
39	1.0000	-.1000	0

(b) Lower surface chordwise row locations

Orifice	x/c	$\frac{y}{b/2}$	z/c
61	0	0.1000	0
62	.0007	.1250	-.0054
63	.0020	.1500	-.0091
64	.0040	.1750	-.0125
65	.0080	.2000	-.0169
66	.0150	.2250	-.0221
67	.0250	.2500	-.0271
68	.0500	.0800	-.0350
69	.1000	.0600	-.0443
70	.1500	.0400	-.0500
71	.2000	.1000	-.0541
72	.2500	.0800	-.0569
73	.3000	.0600	-.0588
74	.3500	.0400	-.0598
75	.4000	.1000	-.0600
76	.4500	.0800	-.0595
77	.5000	.0600	-.0581
79	.6000	.1000	-.0523
80	.6500	.0800	-.0470
81	.7000	.0600	-.0408
82	.7500	.0400	-.0345
83	.8000	.1000	-.0282
84	.8500	.0800	-.0219
85	.9000	.0600	-.0156
86	.9400	.0437	-.0106
87	.9600	.0355	-.0080
88	.9800	.0275	-.0055
90	1.0000	.1000	0

(c) Upper surface spanwise row locations

Orifice	x/c	$\frac{y}{b/2}$	z/c
40	1.0000	-0.8750	0
41	1.0000	-.7500	0
42	1.0000	-.5000	0
44	1.0000	.7500	0
45	1.0000	.8750	0
46	0.8000	-0.8750	0.0282
47	.8000	-.7500	.0282
48	.8000	-.5000	.0282
49	.8000	.5000	.0282
50	.8000	.7500	.0282
51	.8000	.8750	.0282
52	0.9400	-0.8750	0.0106
53	.9400	-.7500	.0106
91	0	0.8750	0
92	0	.9250	0
93	0	.9500	0
94	0	.9750	0

(d) Upper surface chordwise (small diameter) row locations

Orifice	x/c	$\frac{y}{b/2}$	z/c
56	0	0.3000	0
58	.0020	.3500	.0091
59	.0040	.3750	.0125

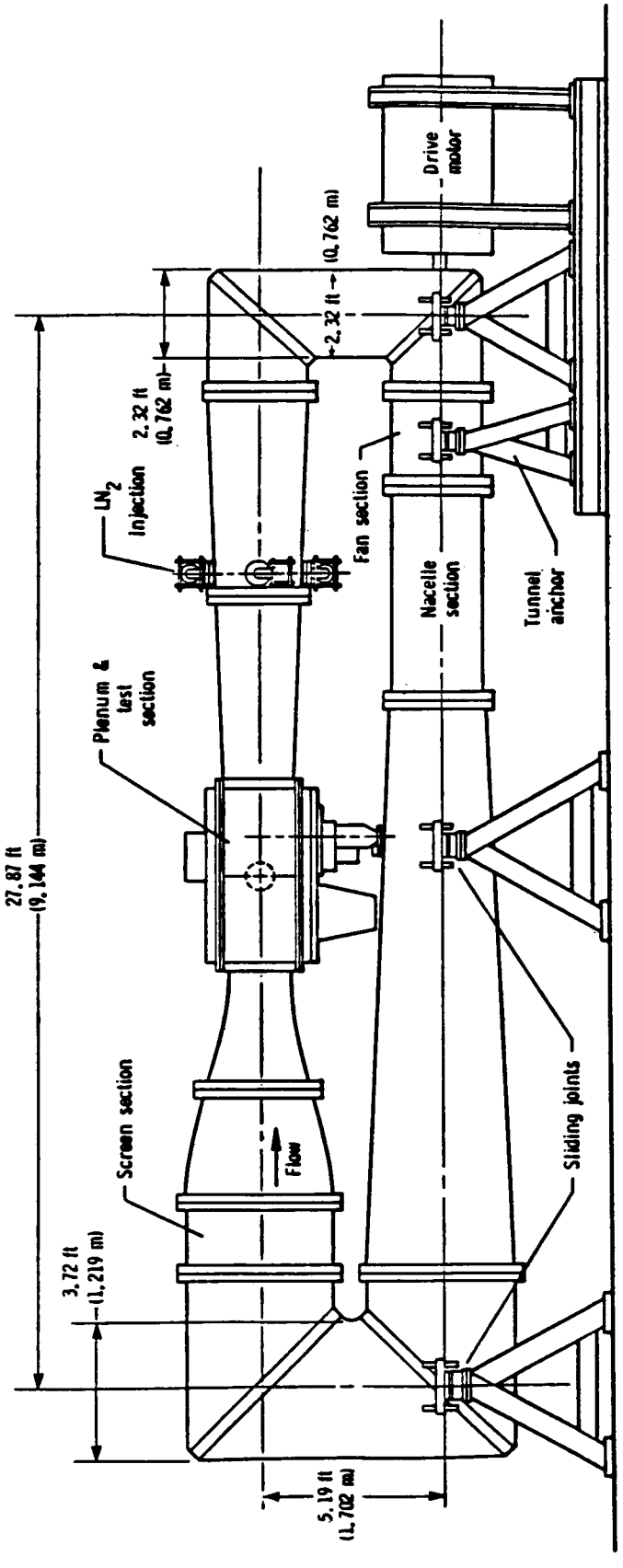

Figure 1.- Schematic diagram of the 0.3-m TCT with the 8-in. by 24-in. two-dimensional test section.

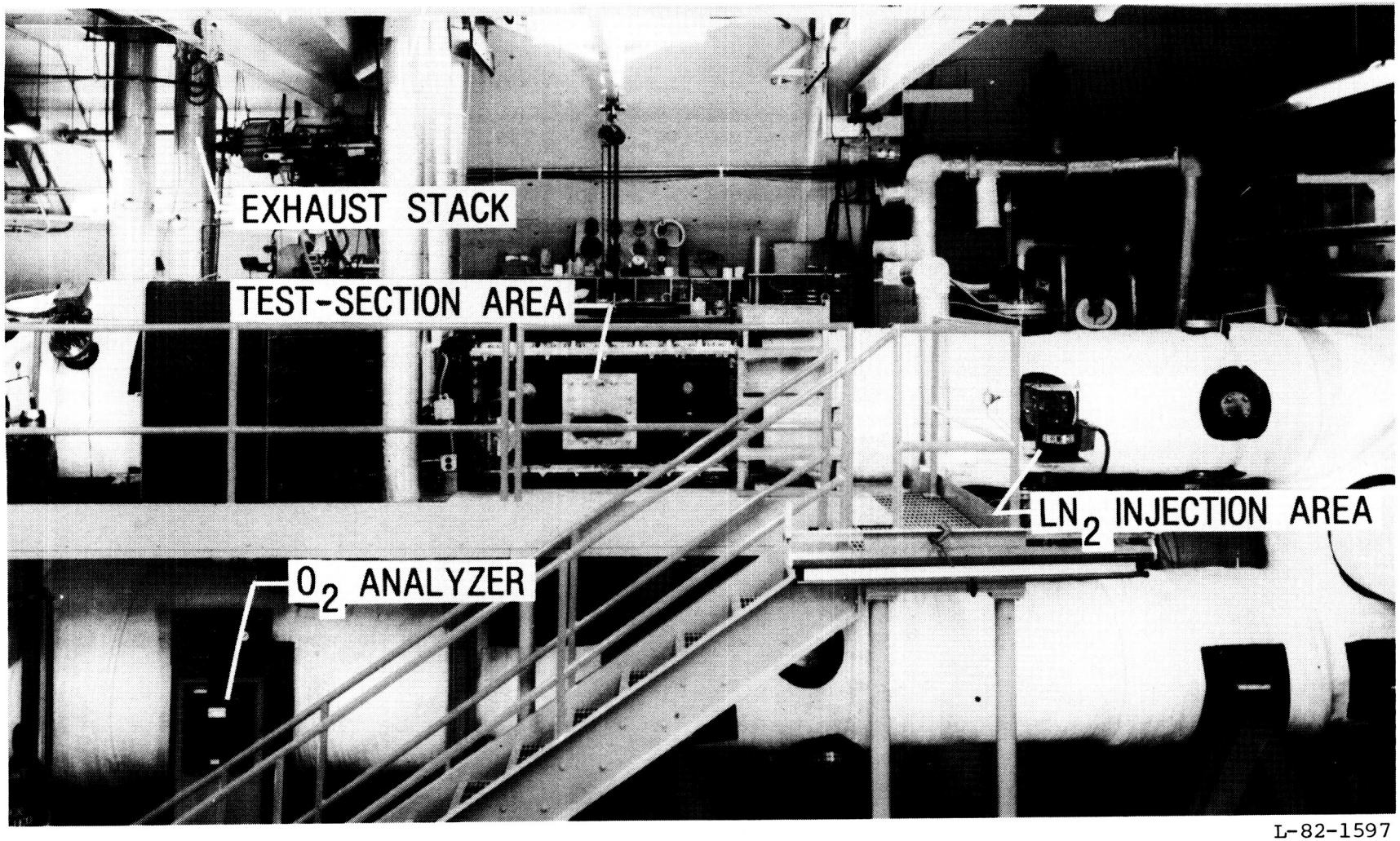

L-82-1597

Figure 2.- Photograph of the 0.3-m TCT with two-dimensional test section.

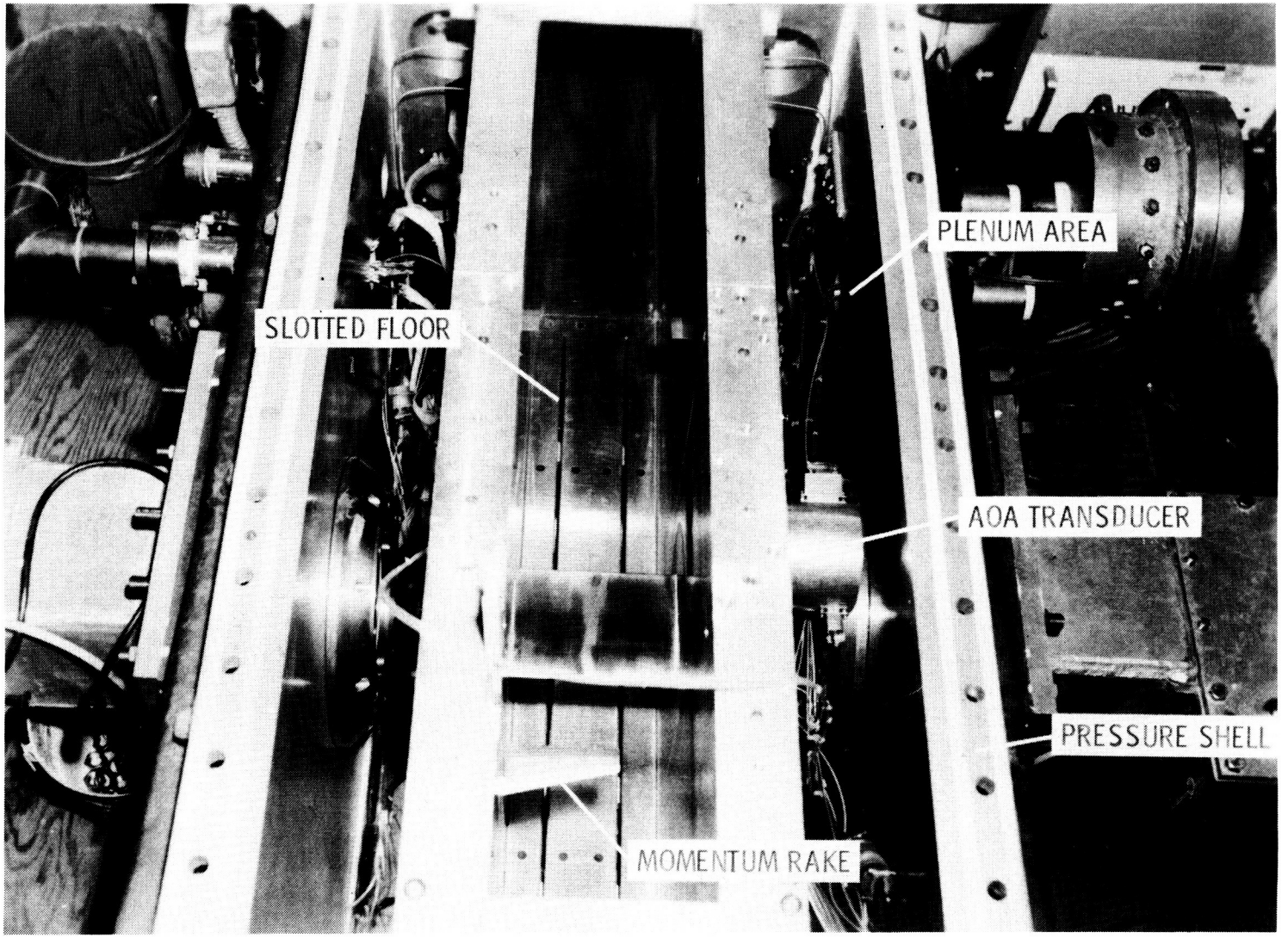

L-79-8913.2

Figure 3.- Photograph of model in the 8-in. by 24-in. two-dimensional test section.

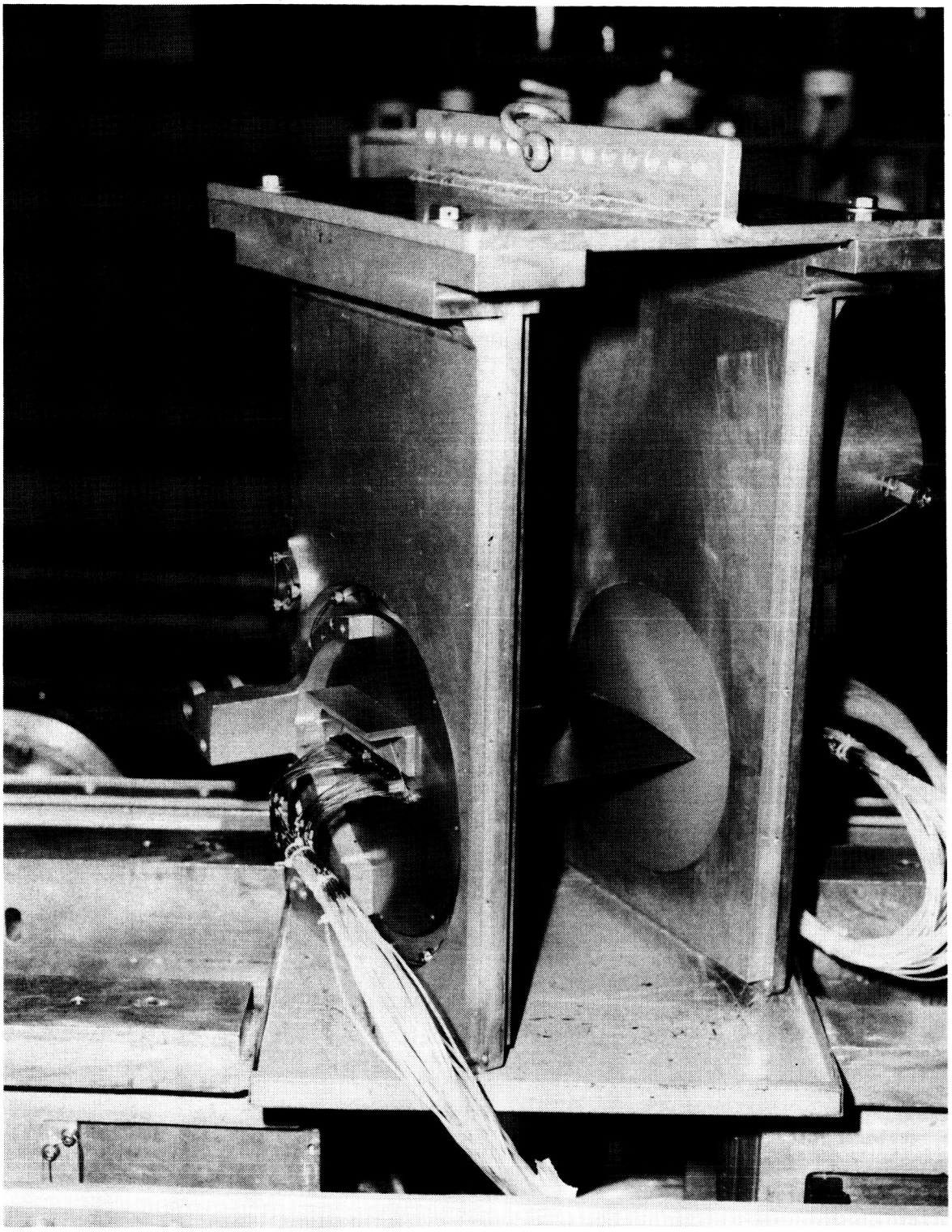

L-84-9448

Figure 4.- Photograph of model mounted between turntables.

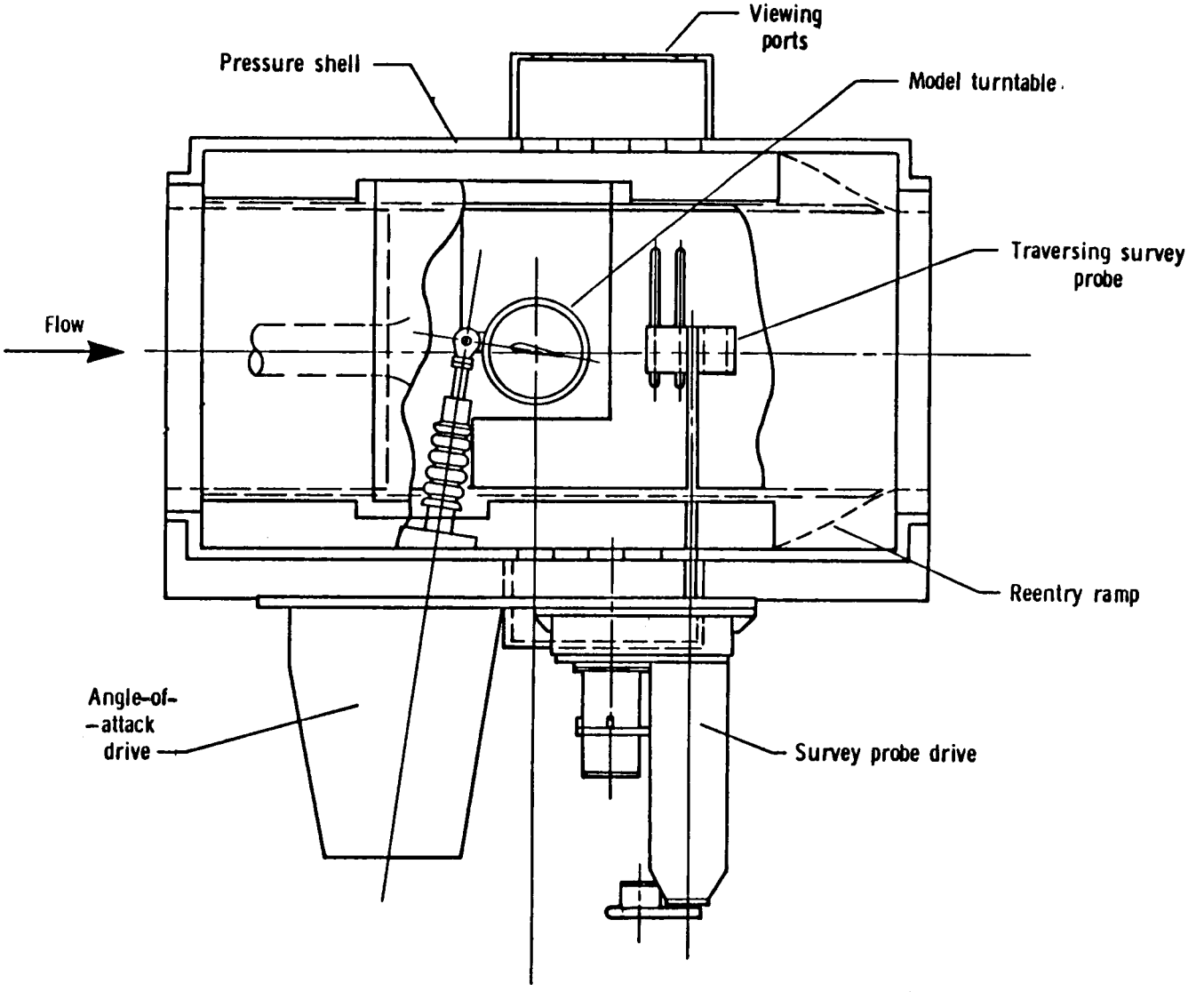

Figure 5.- Sketch of details of the 8-in. by 24-in. two-dimensional test section.

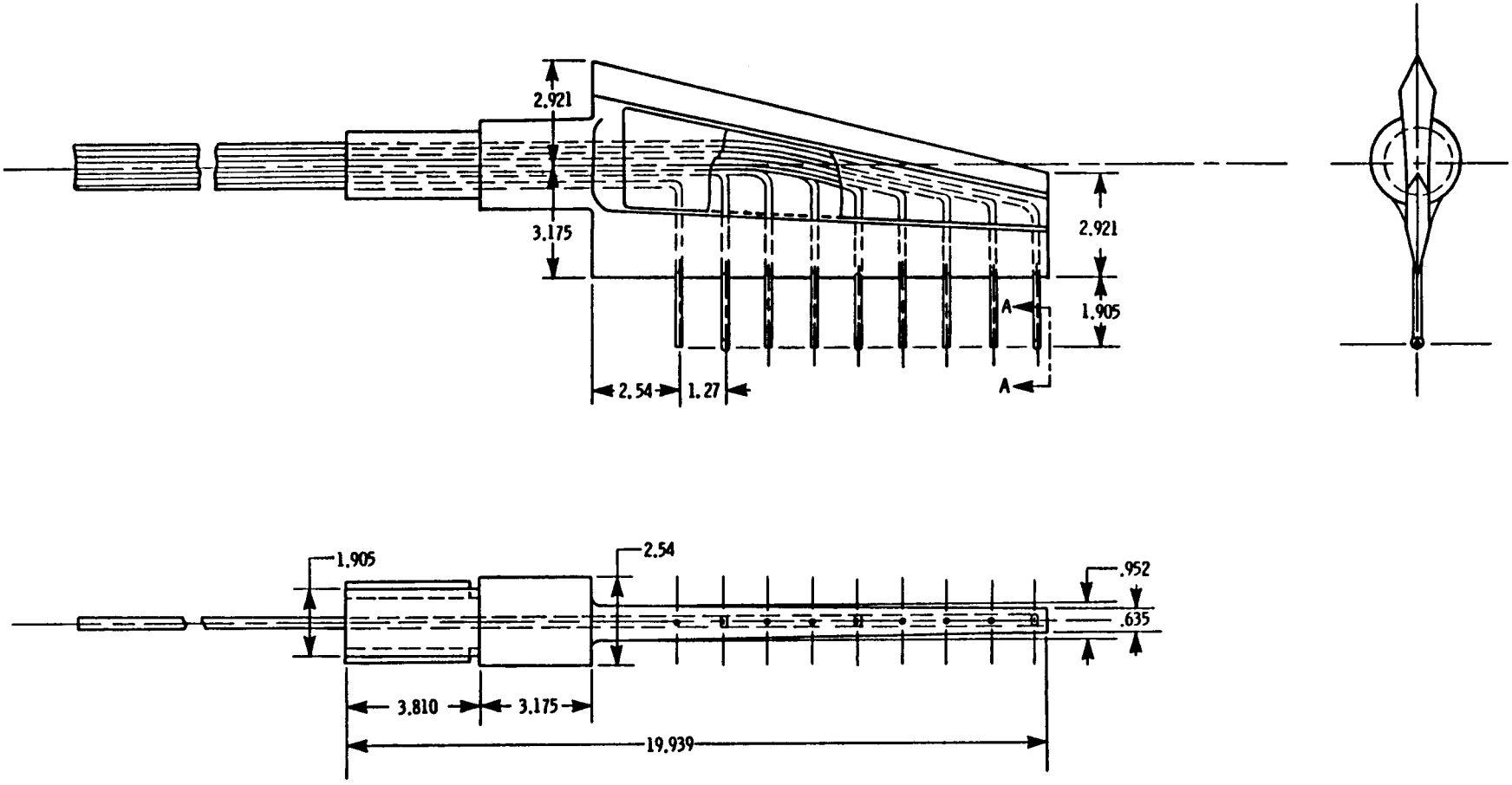

Figure 6.- Sketch of total-pressure probe rake. All dimensions are given in centimeters.

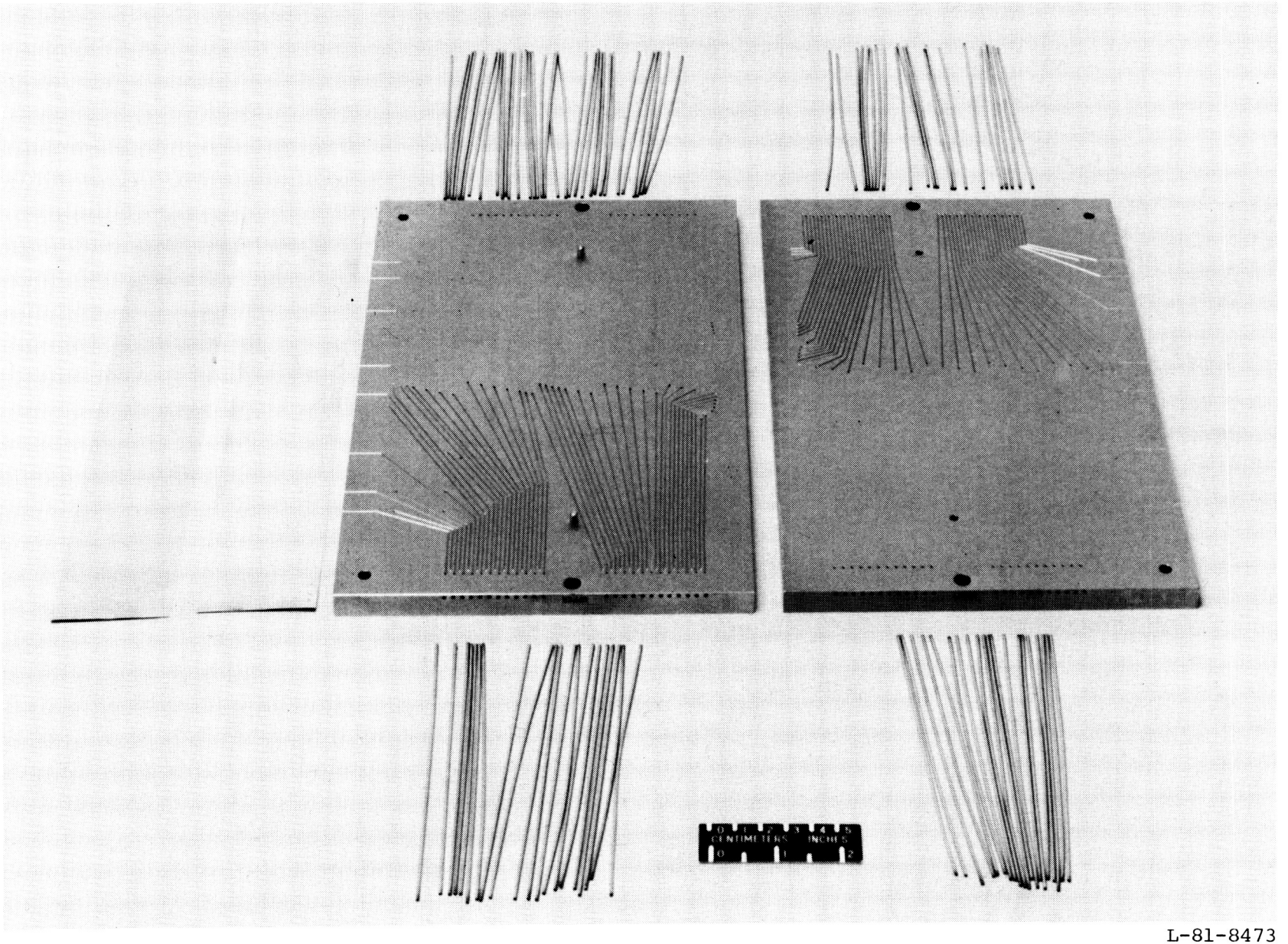

L-81-8473

Figure 7.- Plates, connector tubing, and two of four pieces of brazing foil for symmetrical airfoil model.

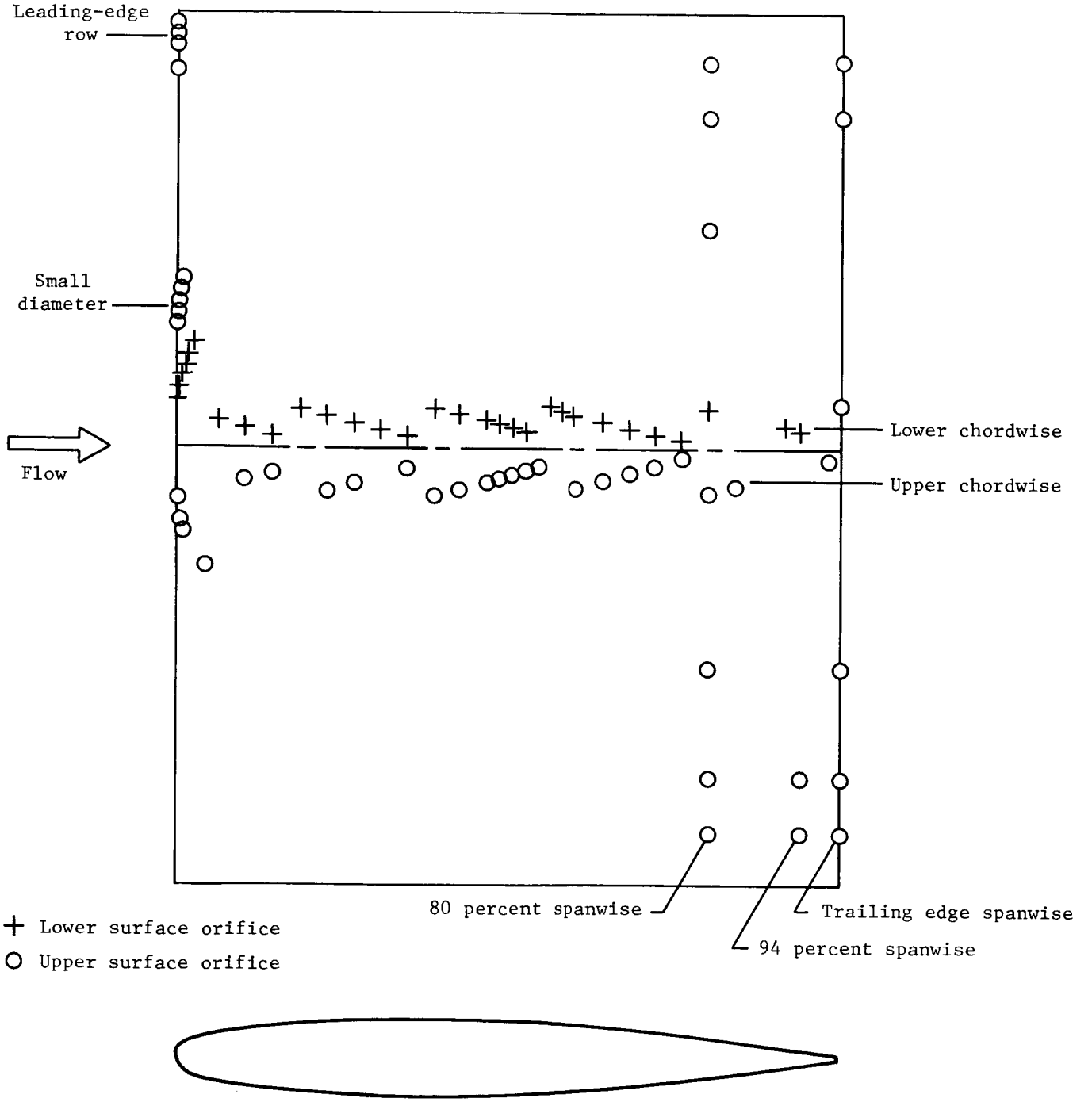

Figure 8.- Layout of pressure orifices on model.

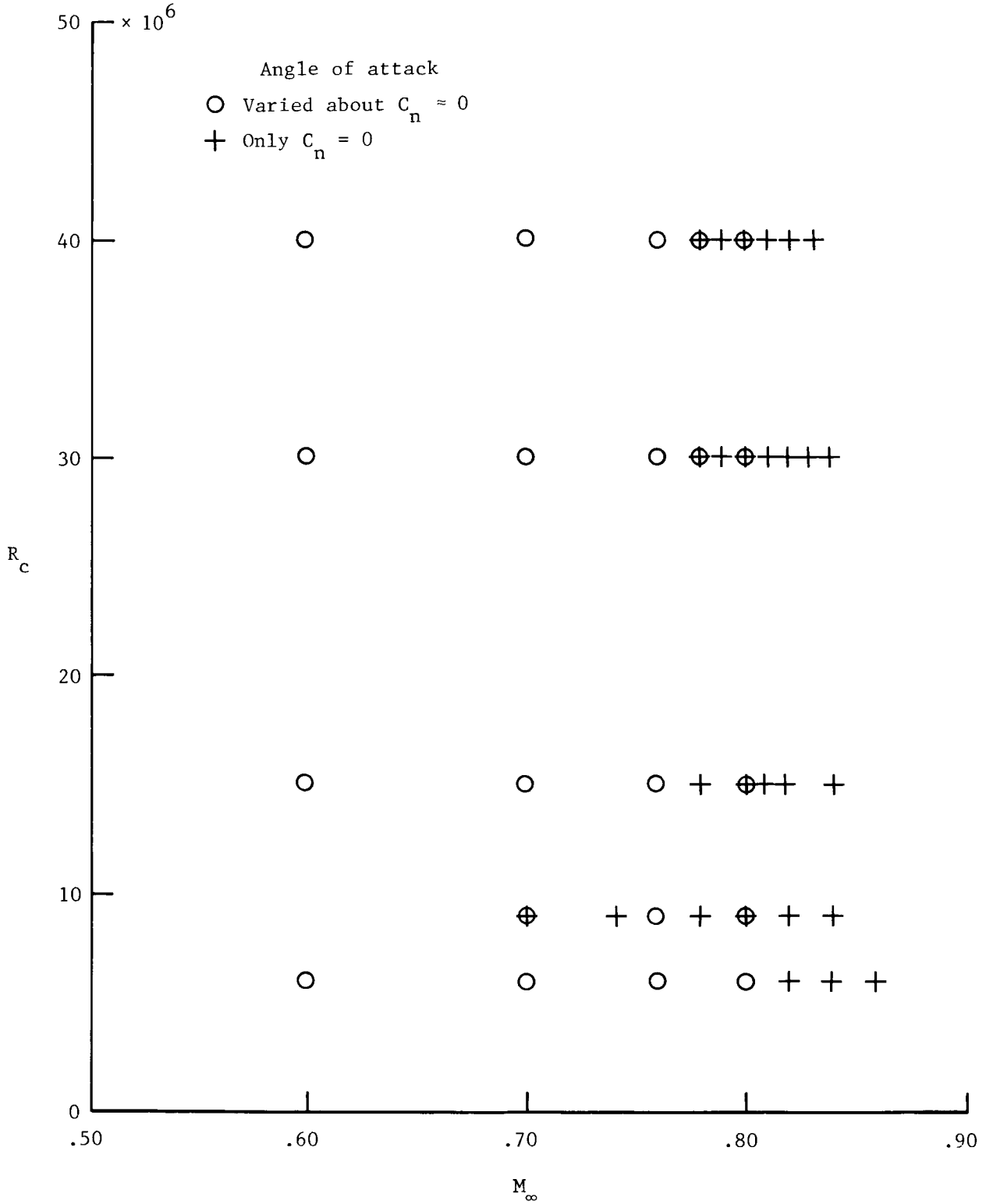

Figure 9.- Matrix of test conditions used.

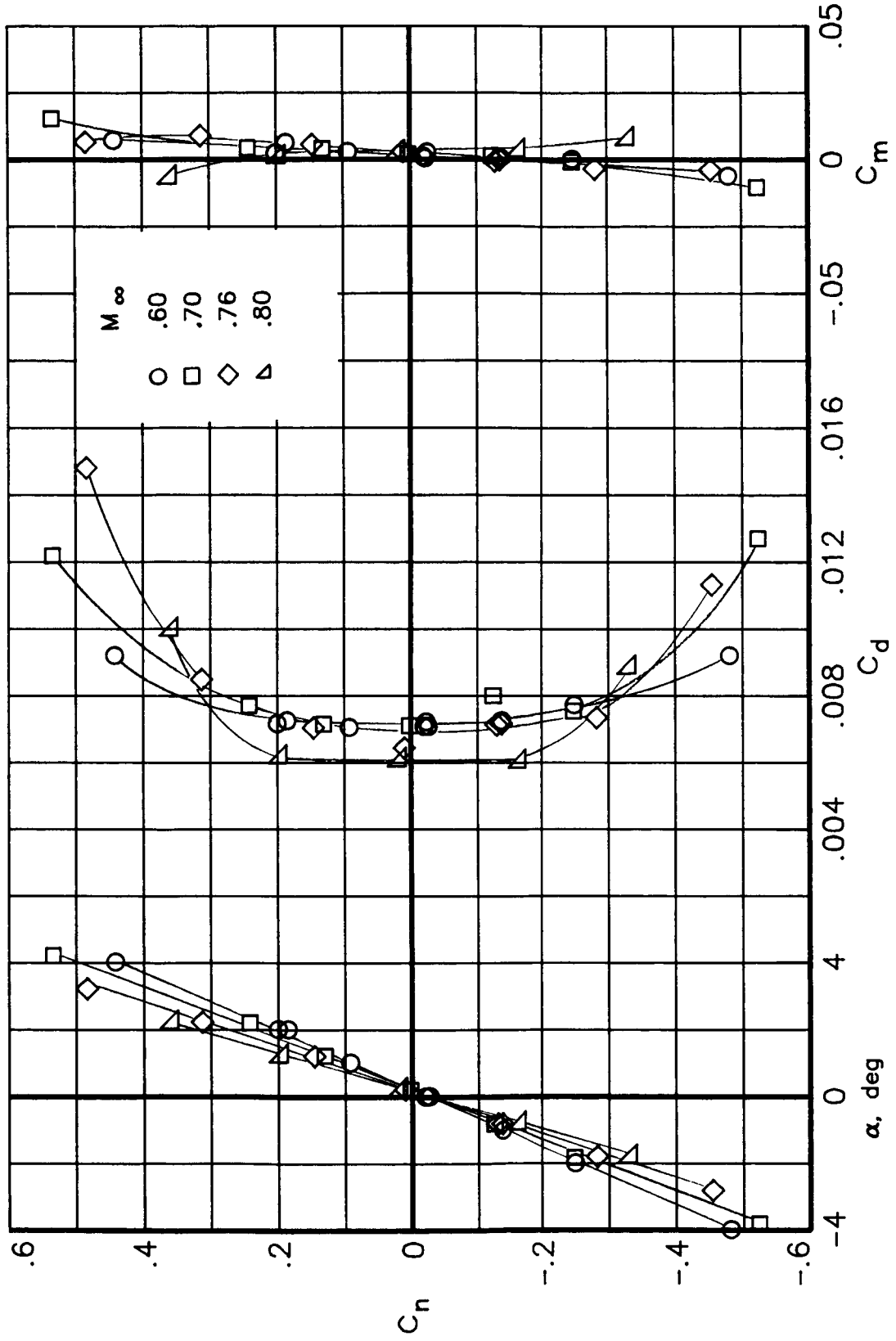

(a) $R_c = 6 \times 10^6$.

Figure 10.- Effect of Mach number on integrated force and moment coefficients.

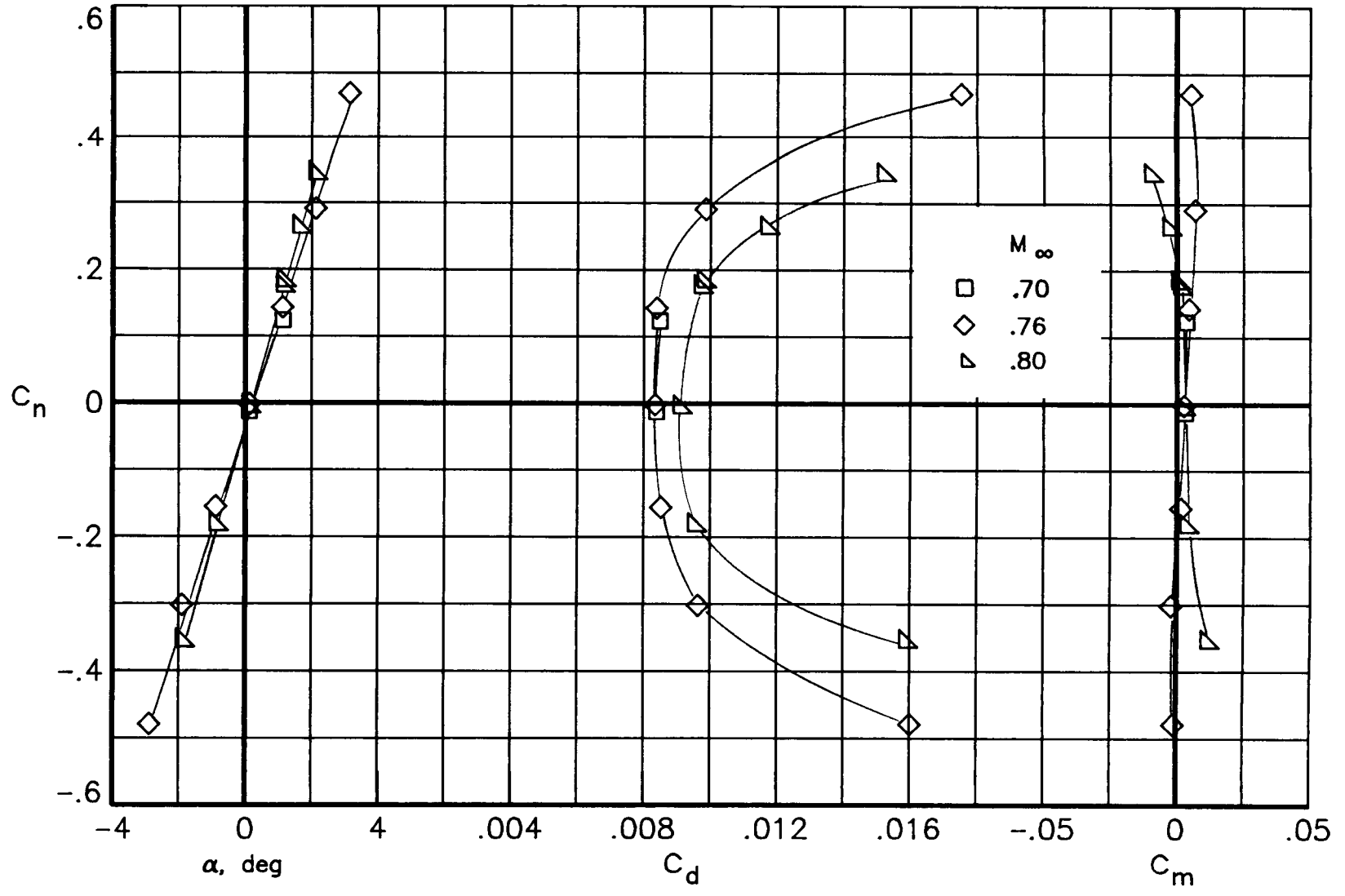

(b) $R_c = 9 \times 10^6$.

Figure 10.- Continued.

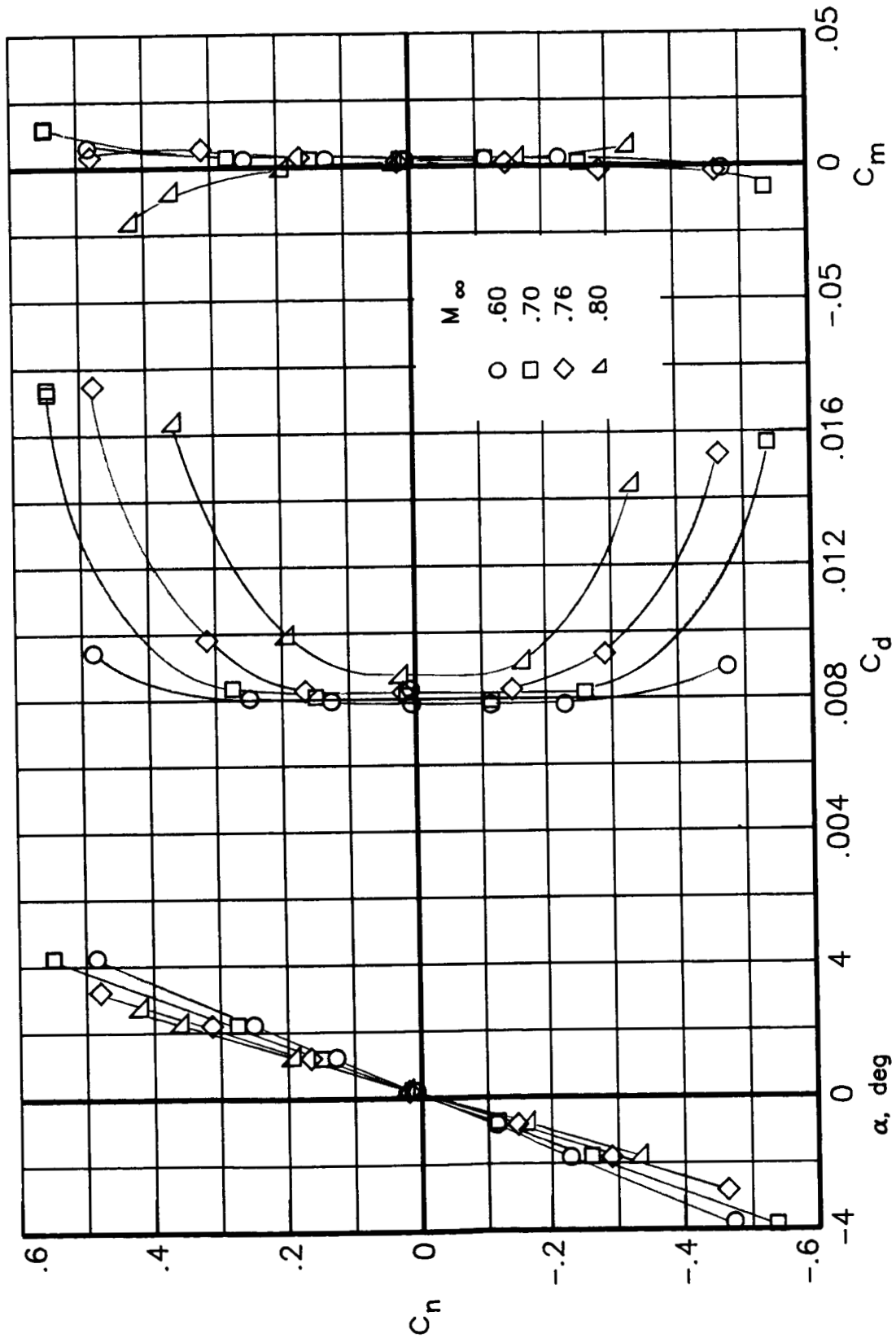

(c) $R_c = 15 \times 10^6$.

Figure 10.- Continued.

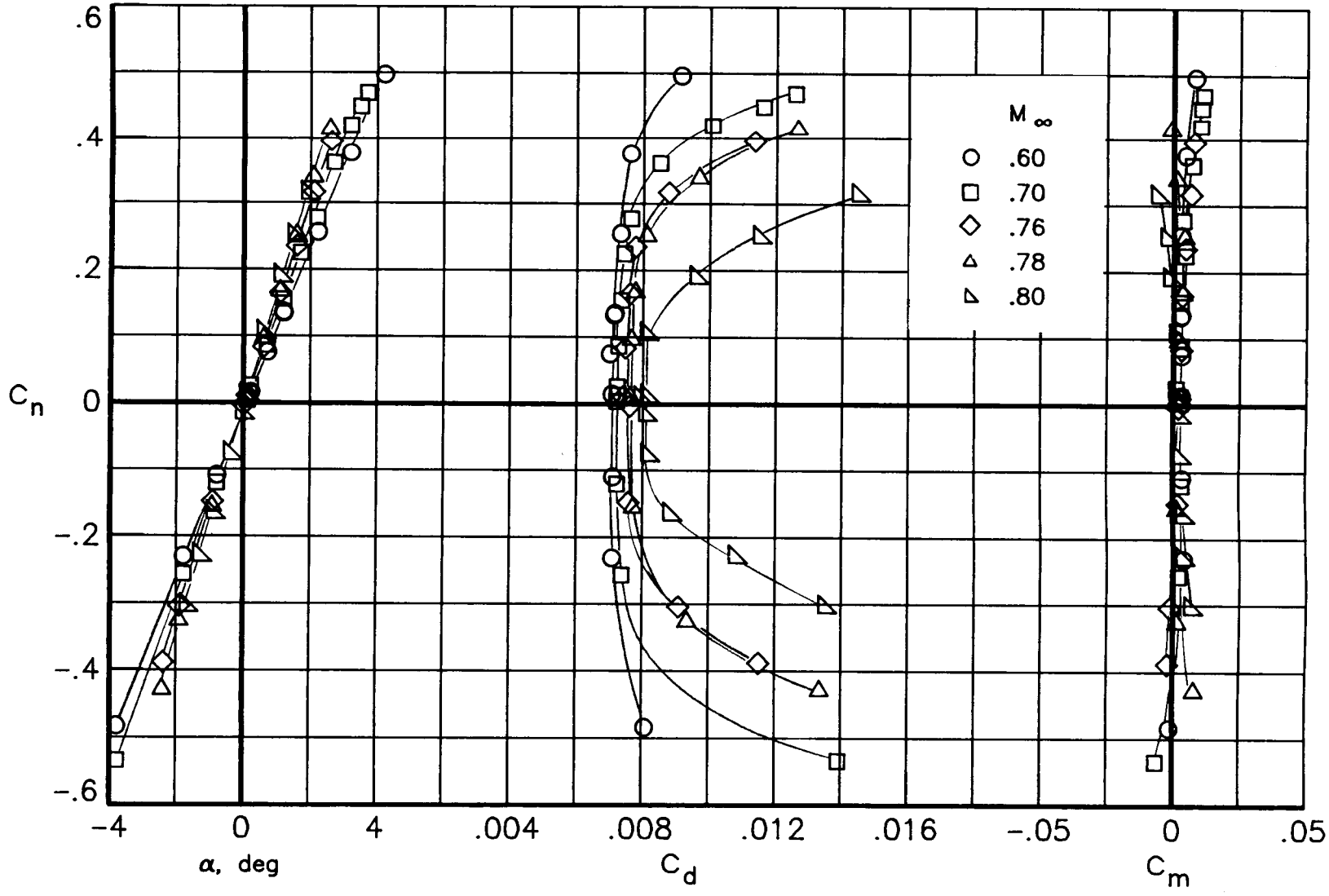

(d) $R_c = 30 \times 10^6$.

Figure 10.- Continued.

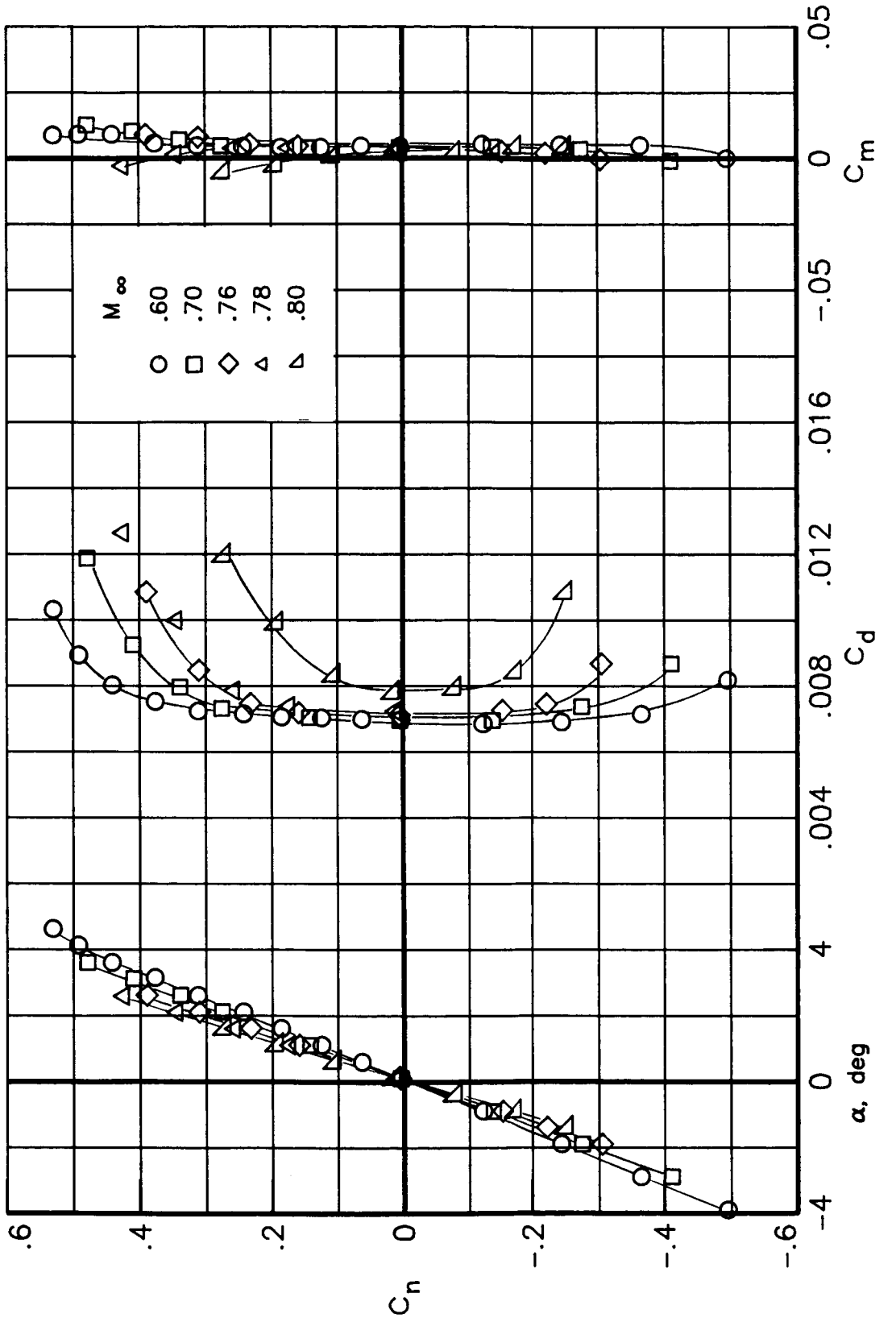

(e) $R_c = 40 \times 10^6$.

Figure 10.- Concluded.

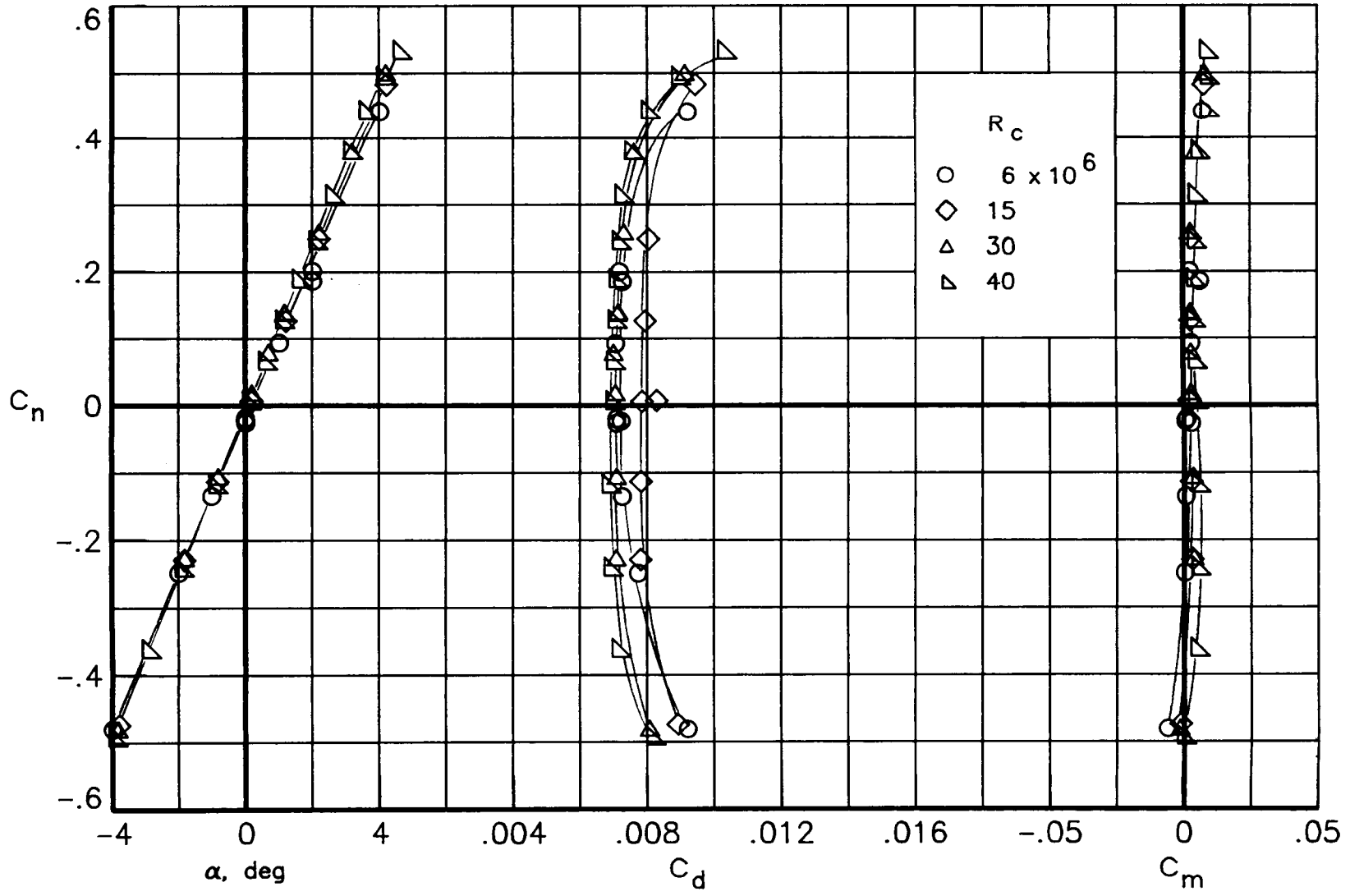

(a) $M_\infty = 0.60$.

Figure 11.- Effect of Reynolds number on integrated force and moment coefficients.

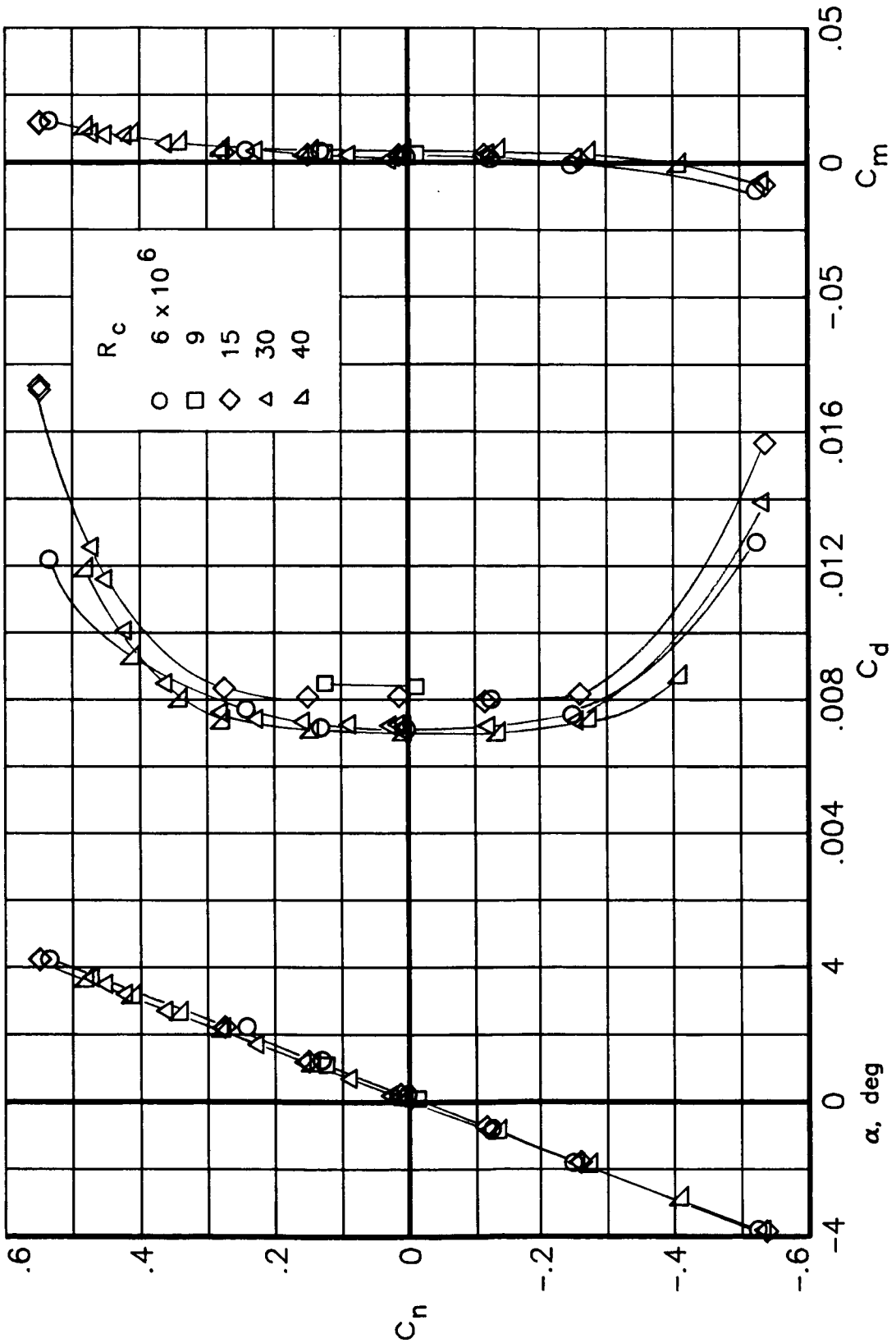

(b) $M_\infty = 0.70$.

Figure 11.- Continued.

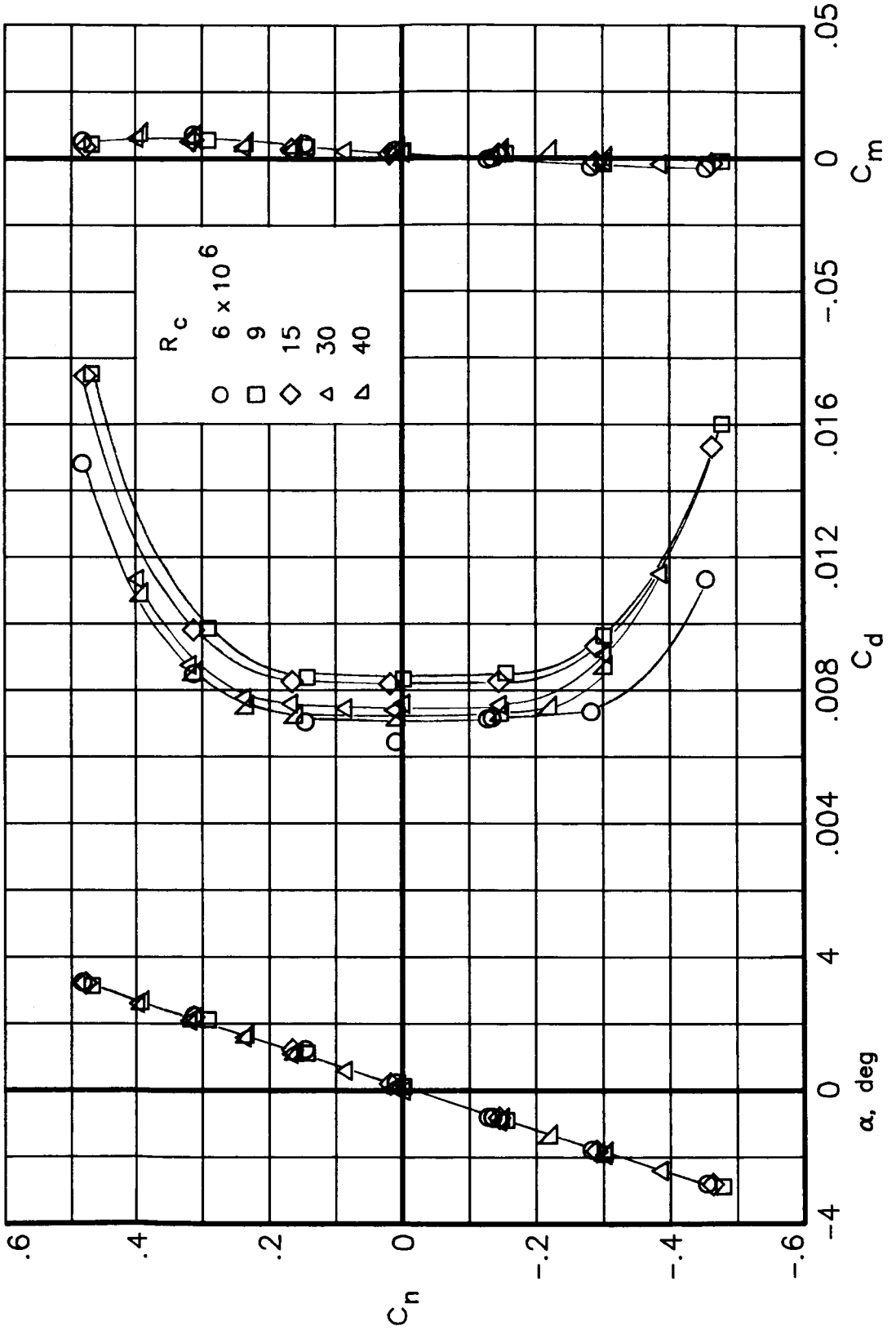

(c) $M_\infty = 0.76$.

Figure 11.- Continued.

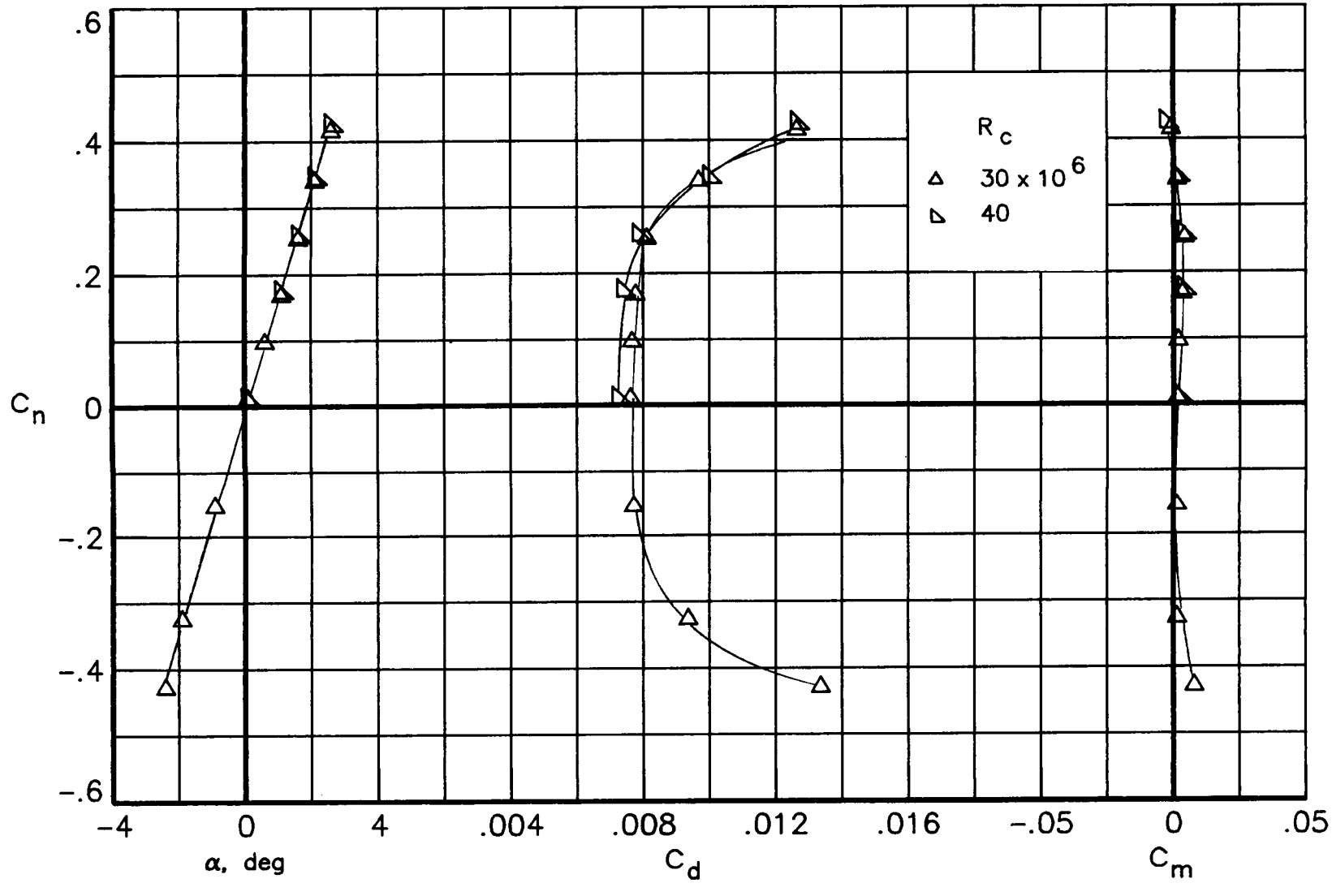

(d) $M_\infty = 0.78$.

Figure 11.- Continued.

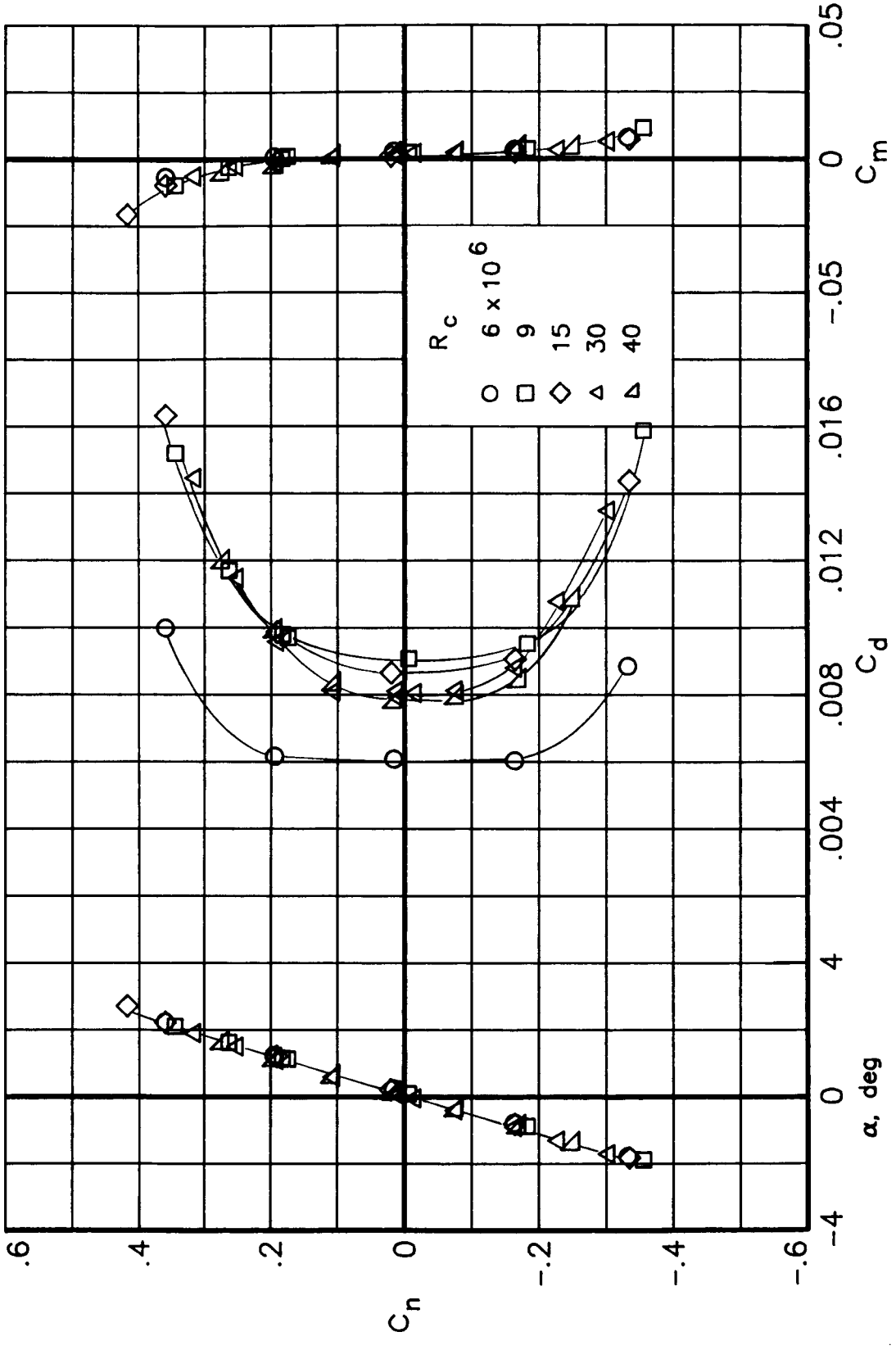

(e) $M_\infty = 0.80$.

Figure 11.- Concluded.

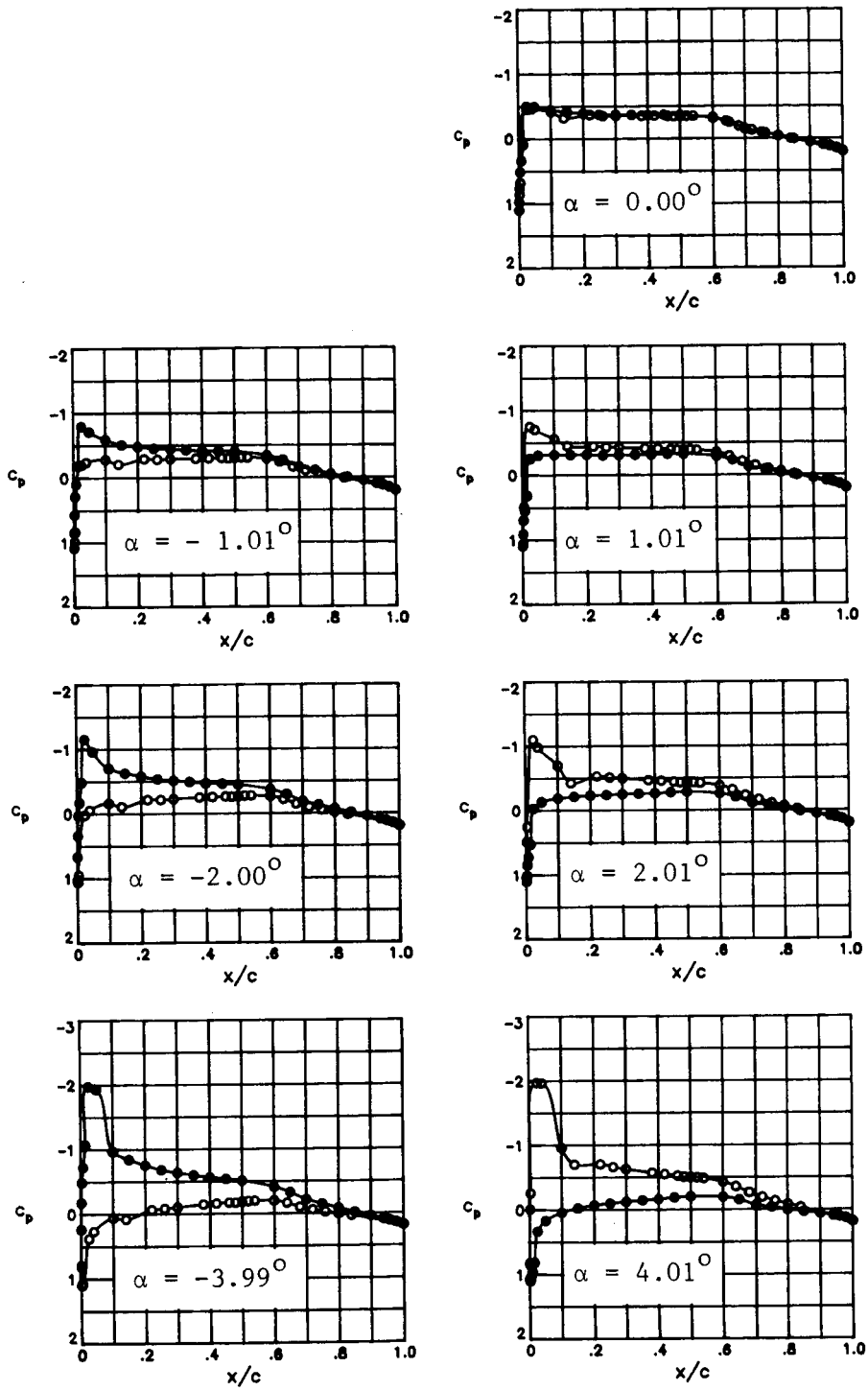

(a) $M_\infty = 0.60$.

Figure 12.- Effect of angle of attack on chordwise pressure distribution at $R_C = 6 \times 10^6$. Open symbols denote upper surface; solid symbols denote lower surface.

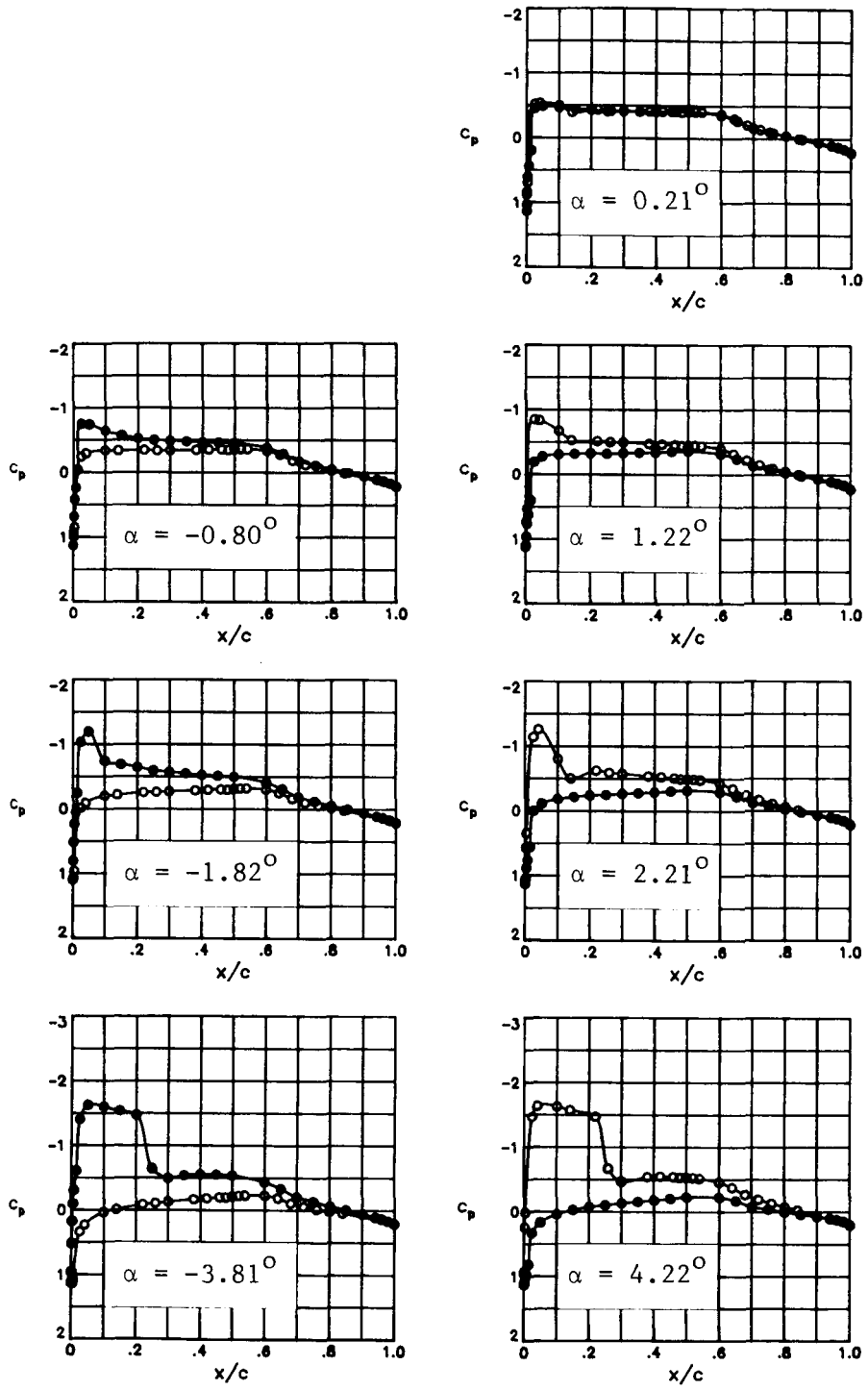

(b) $M_\infty = 0.70$.

Figure 12.- Continued.

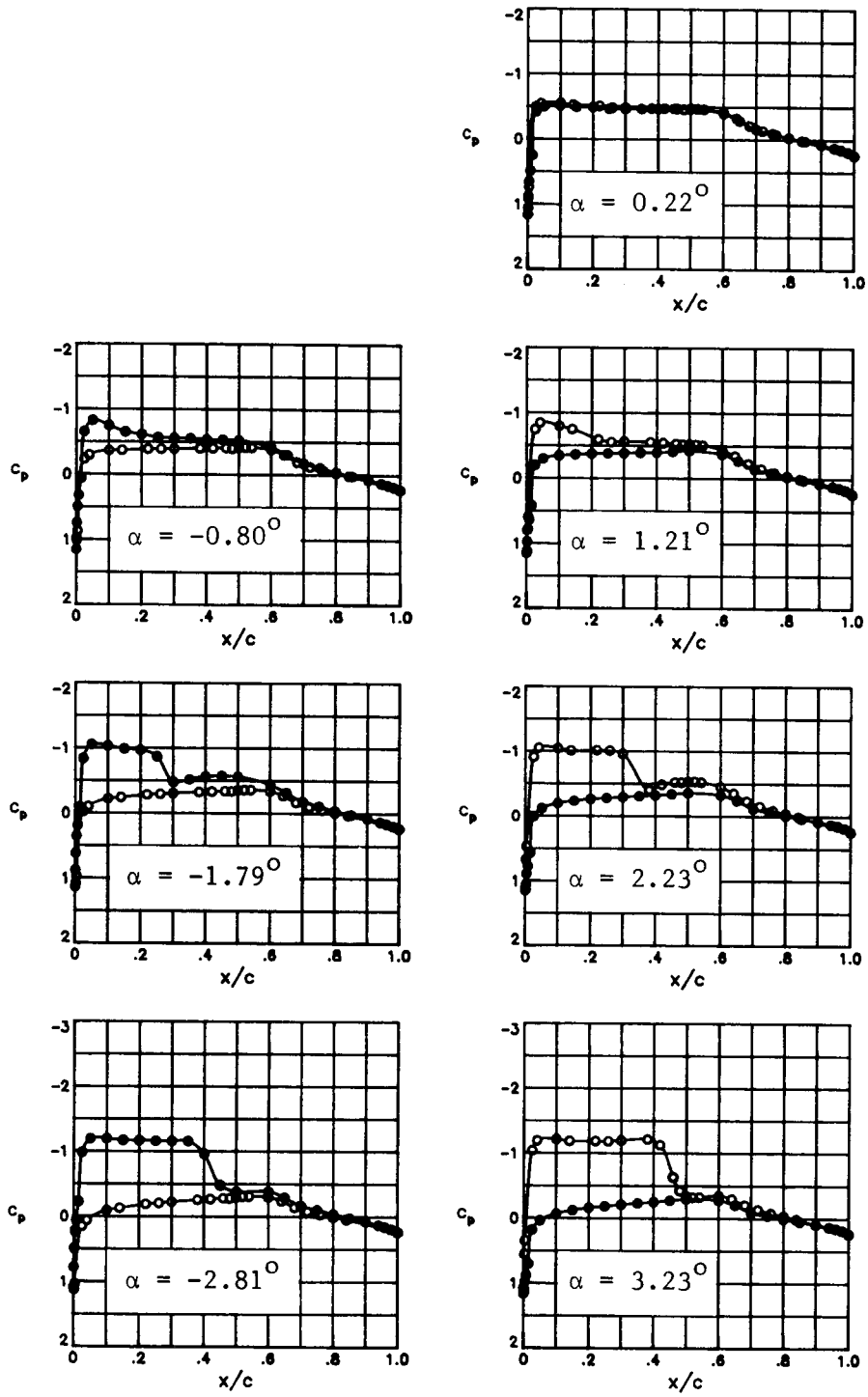

(c) $M_\infty = 0.76$.

Figure 12.- Continued.

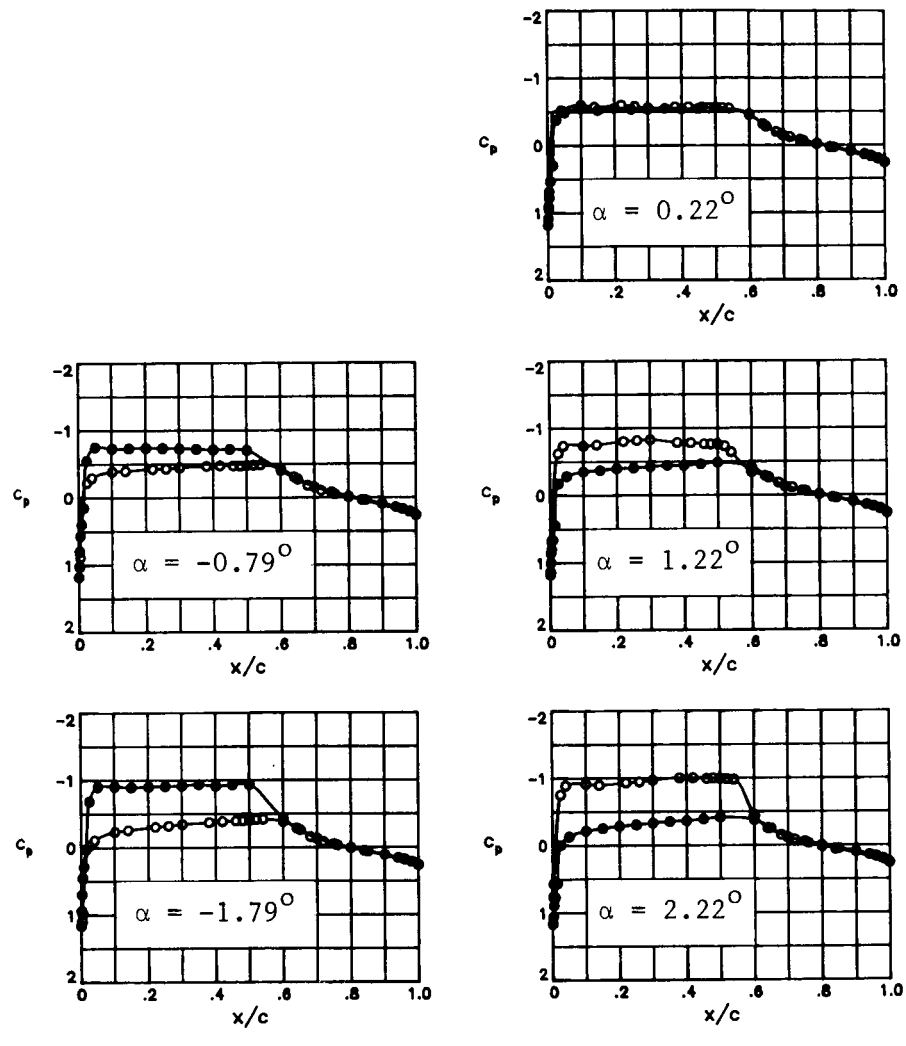

(d) $M_\infty = 0.80$.

Figure 12.- Concluded.

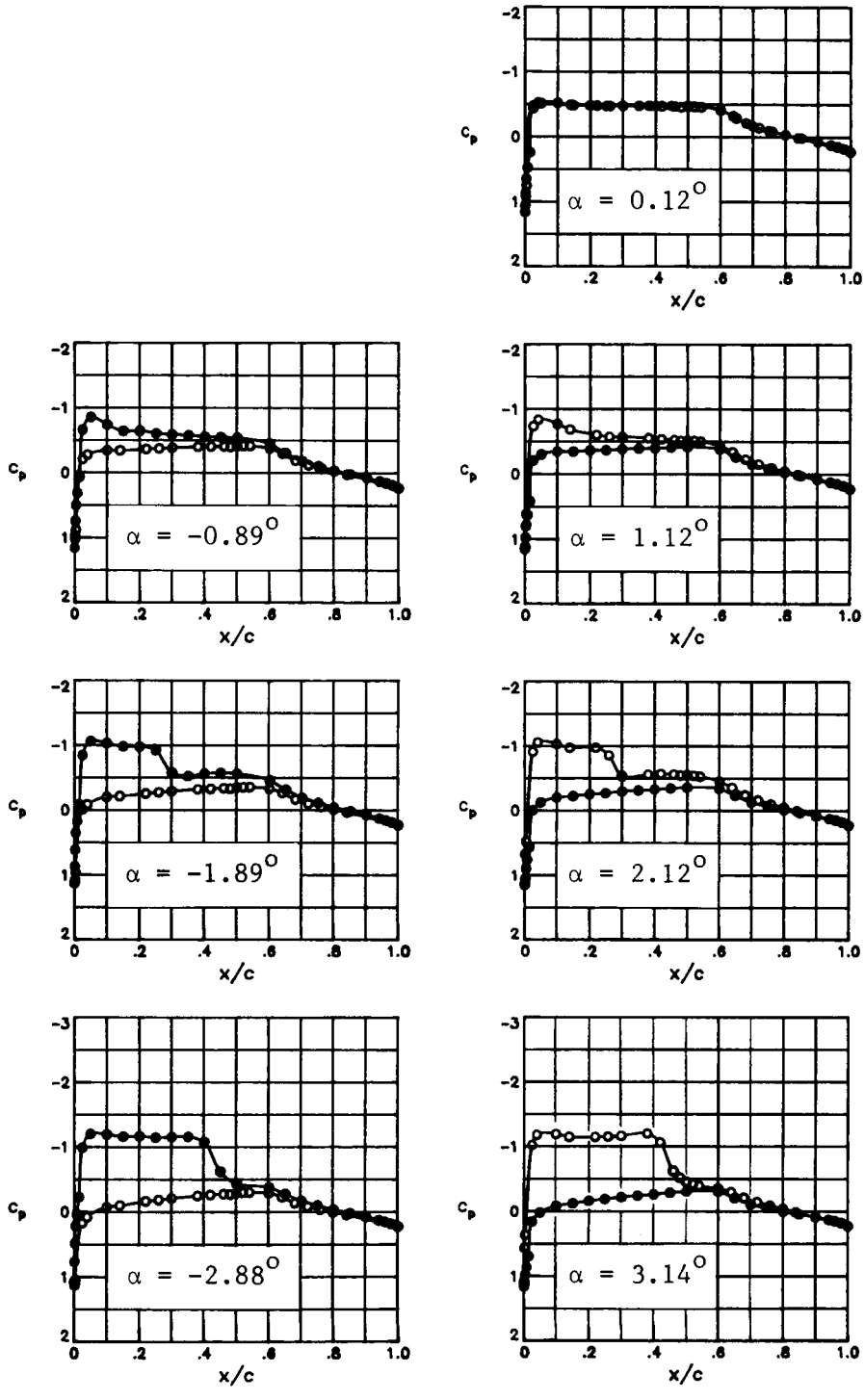

(a) $M_\infty = 0.76$.

Figure 13.- Effect of angle of attack on chordwise pressure distribution at $R_c = 9 \times 10^6$. Open symbols denote upper surface; solid symbols denote lower surface.

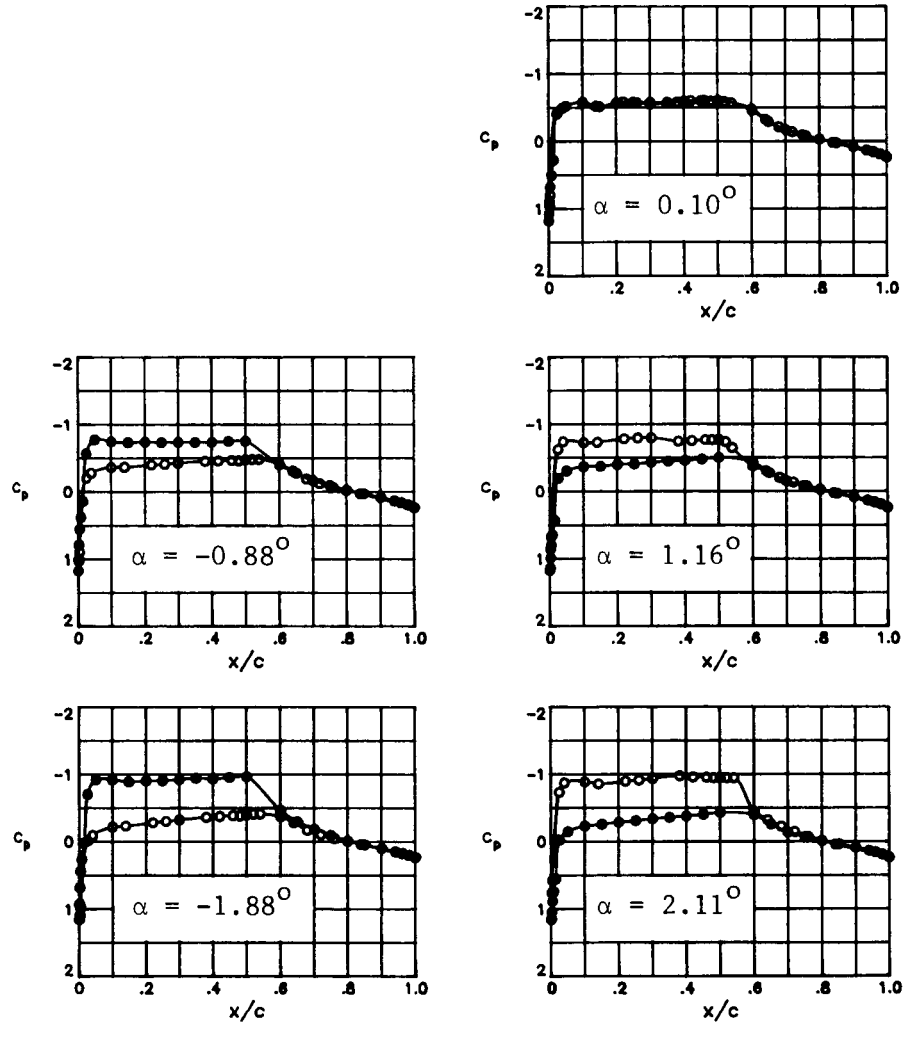

(b) $M_\infty = 0.80$.

Figure 13.- Concluded.

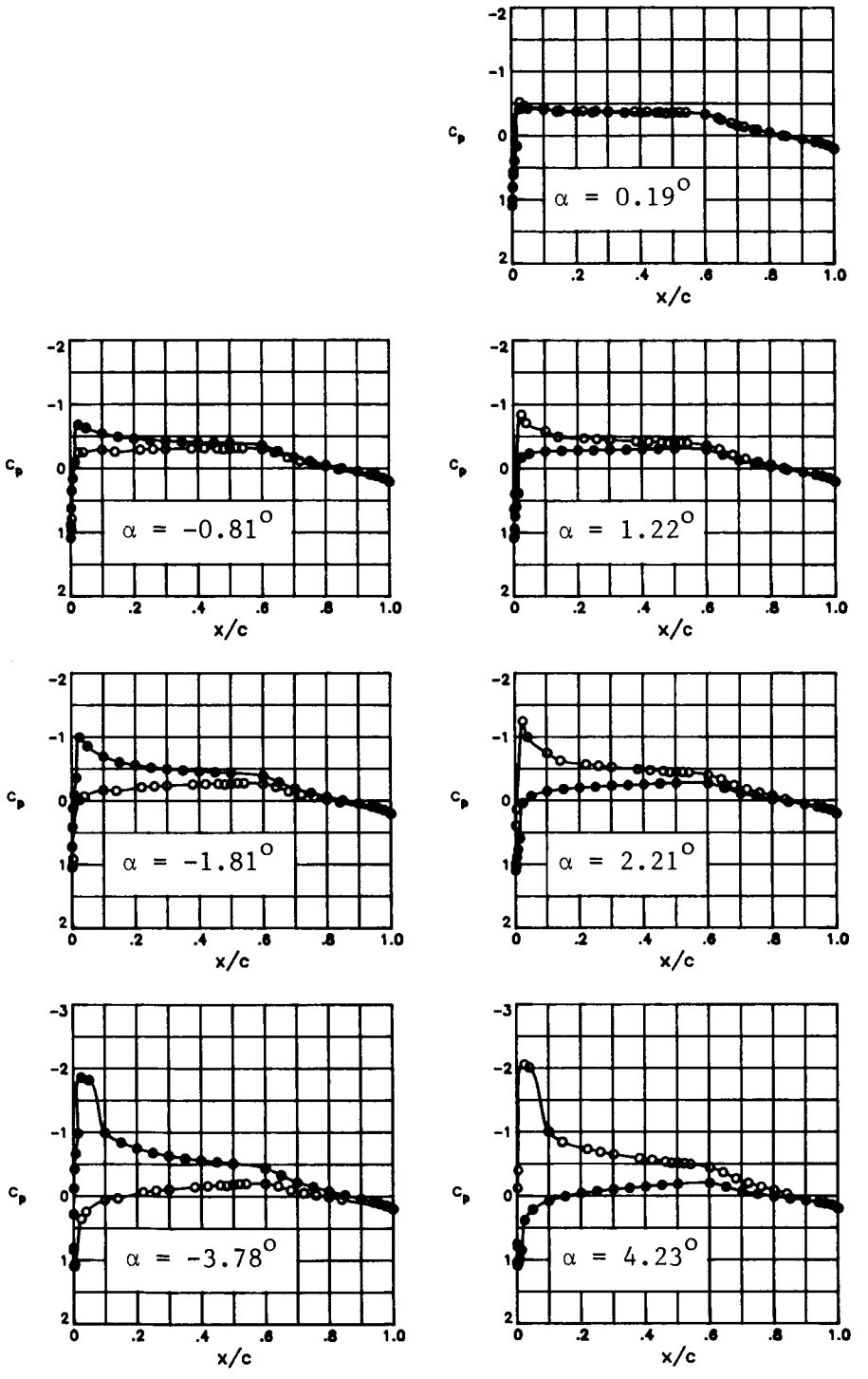

(a) $M_\infty = 0.60$.

Figure 14.- Effect of angle of attack on chordwise pressure distribution at $R_c = 15 \times 10^6$. Open symbols denote upper surface; solid symbols denote lower surface.

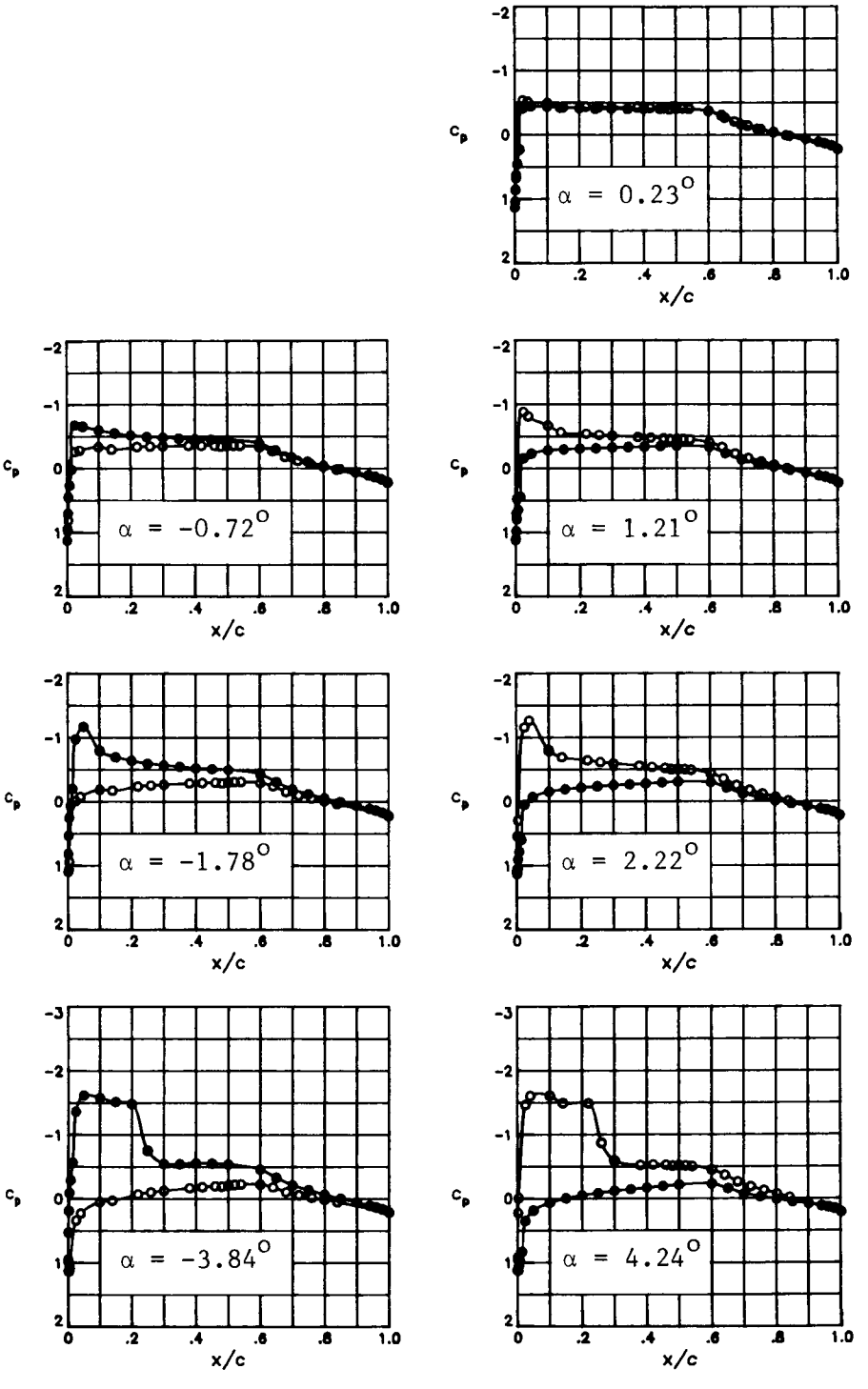

(b) $M_\infty = 0.70$.

Figure 14.- Continued.

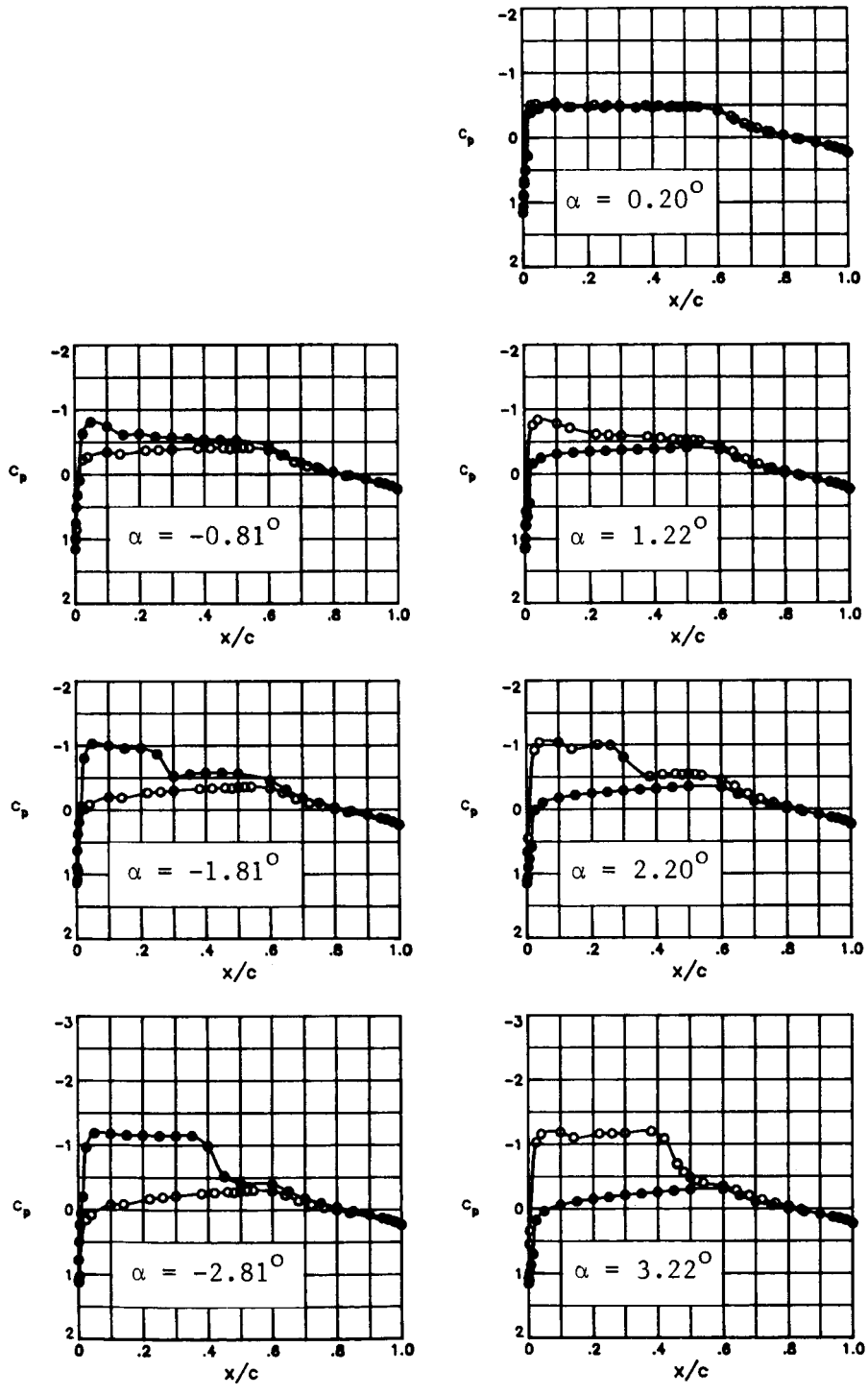

(c) $M_\infty = 0.76$.

Figure 14.- Continued.

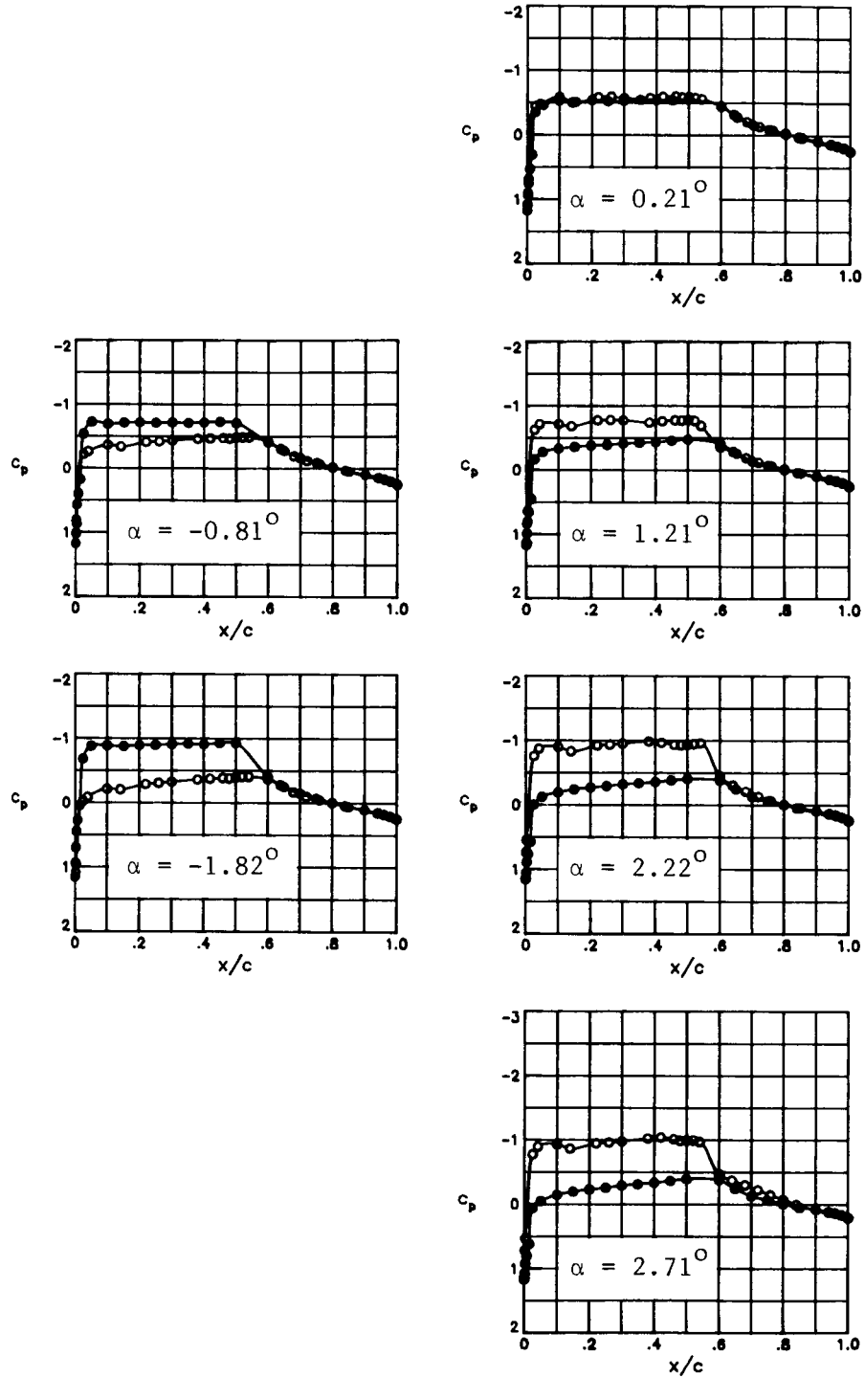

(d) $M_\infty = 0.80$.

Figure 14.- Concluded.

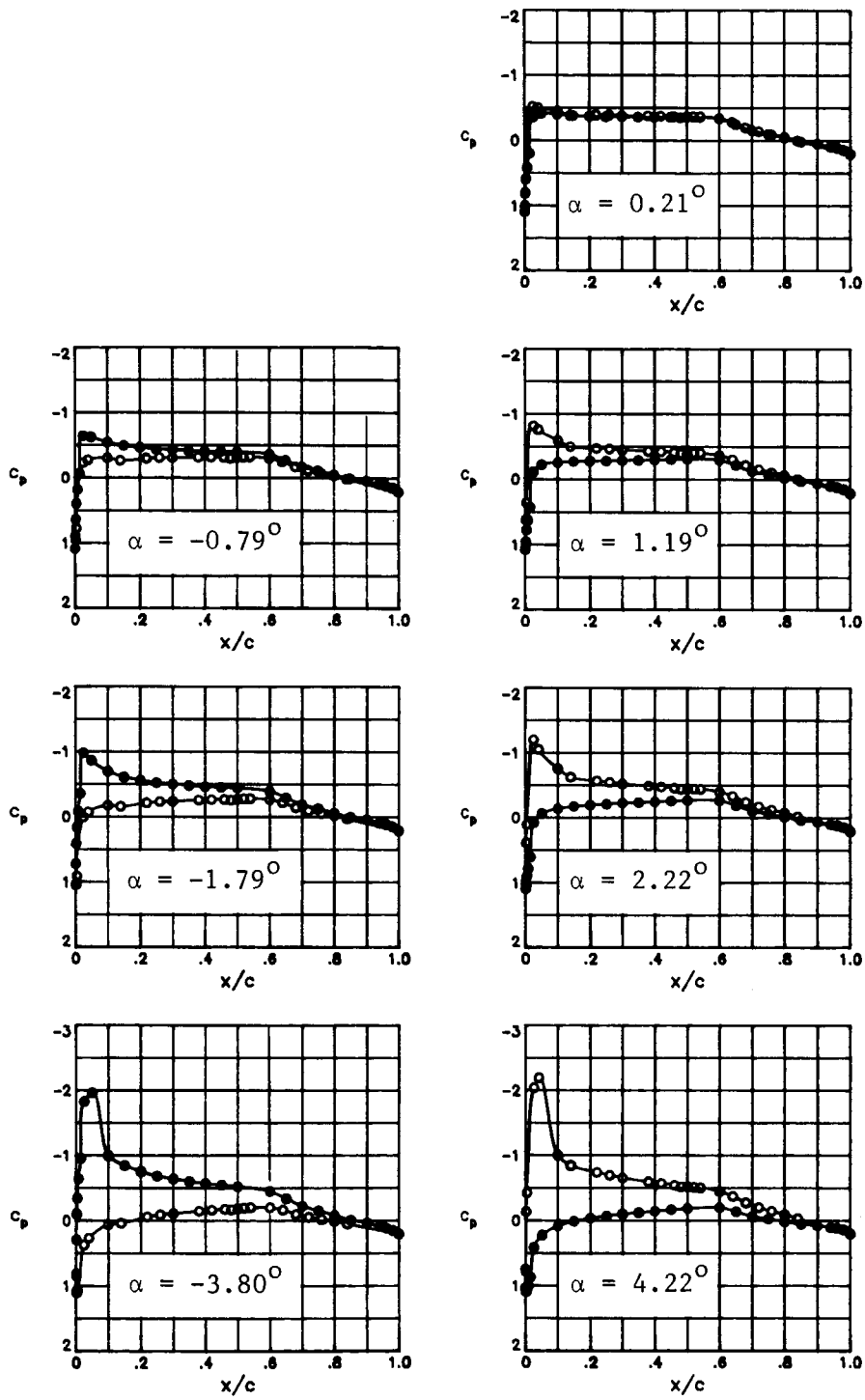

(a) $M_\infty = 0.60$.

Figure 15.- Effect of angle of attack on chordwise pressure distribution at $R_C = 30 \times 10^6$. Open symbols denote upper surface; solid symbols denote lower surface.

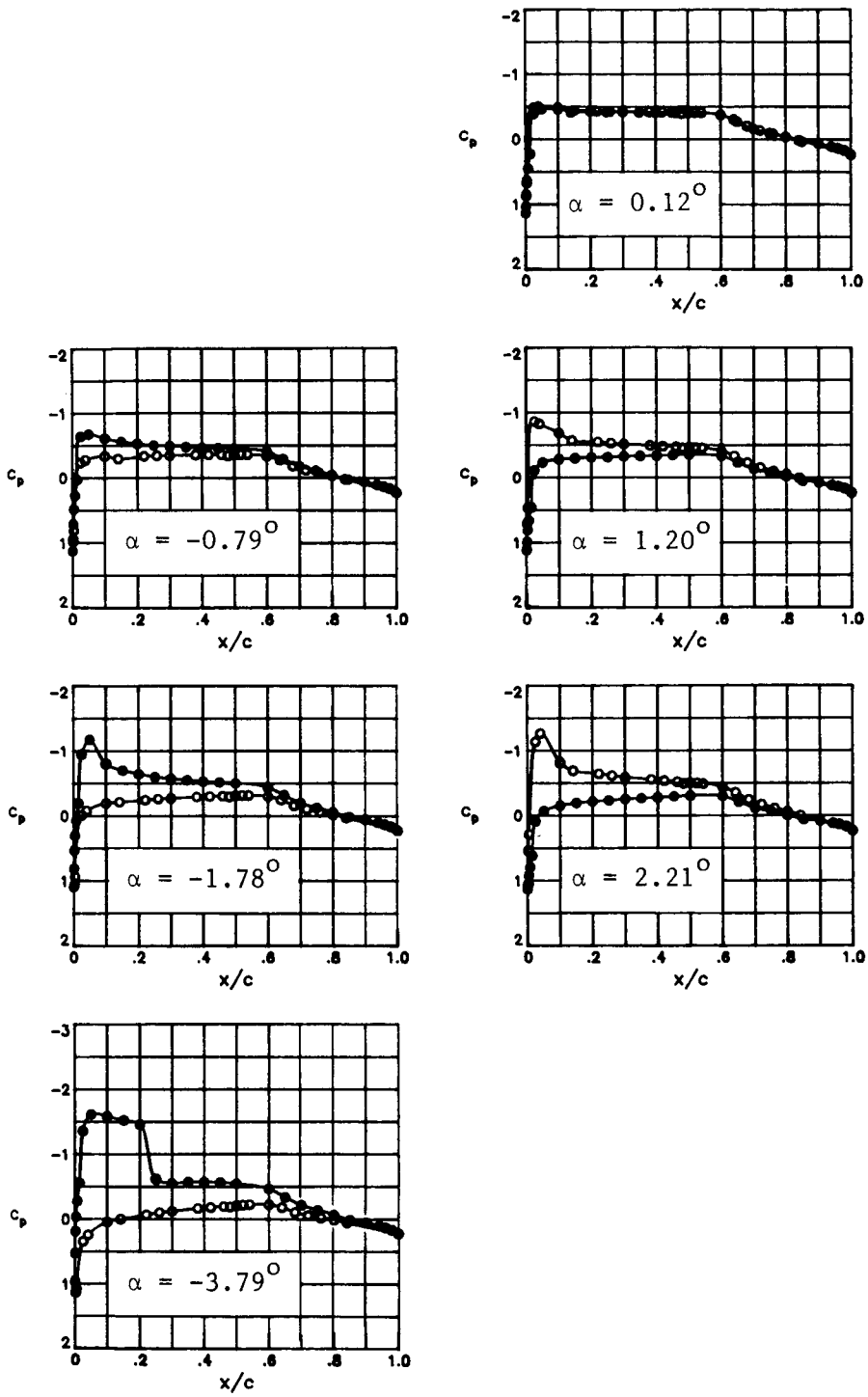

(b) $M_\infty = 0.70$.

Figure 15.- Continued.

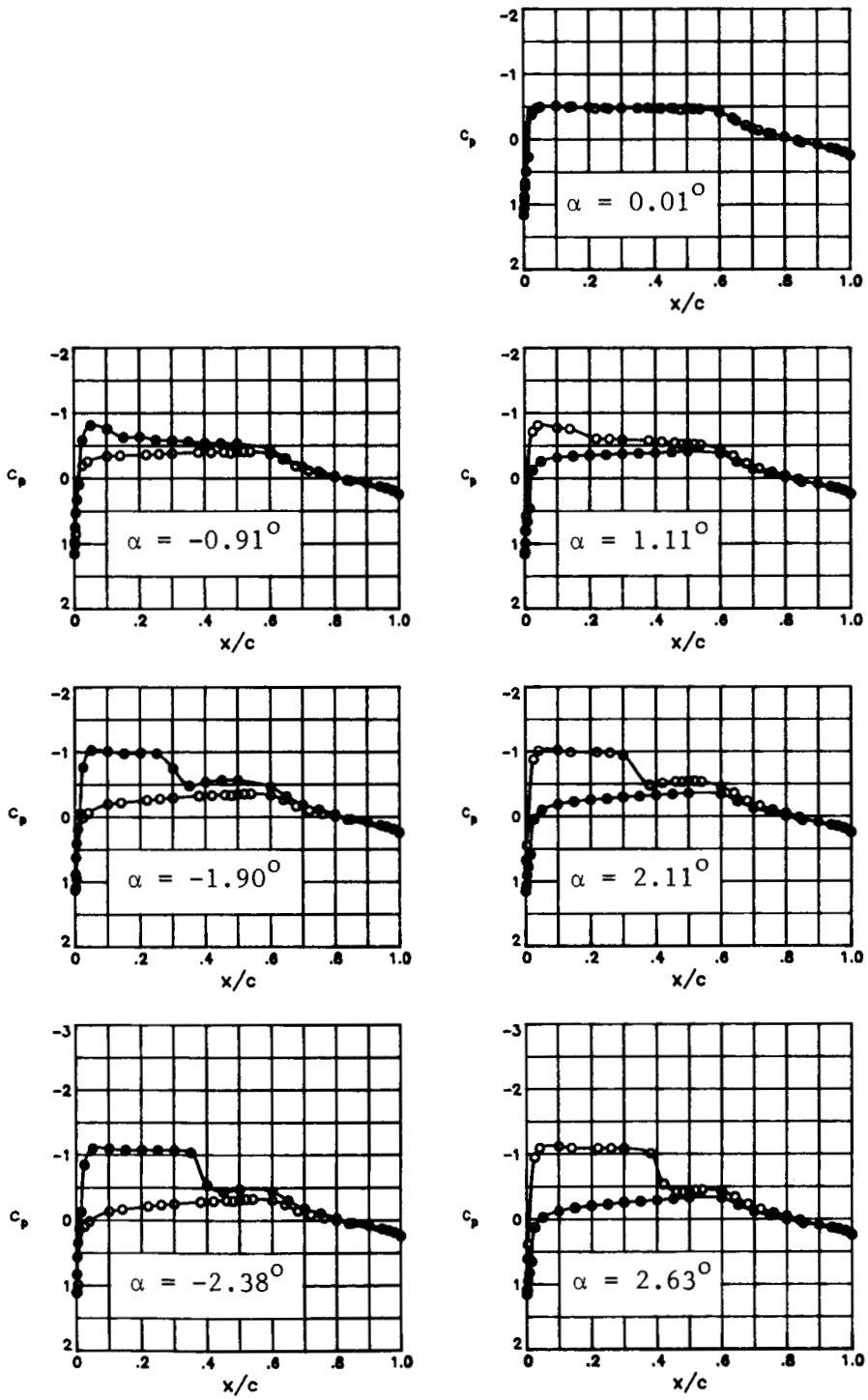

(c) $M_\infty = 0.76$.

Figure 15.- Continued.

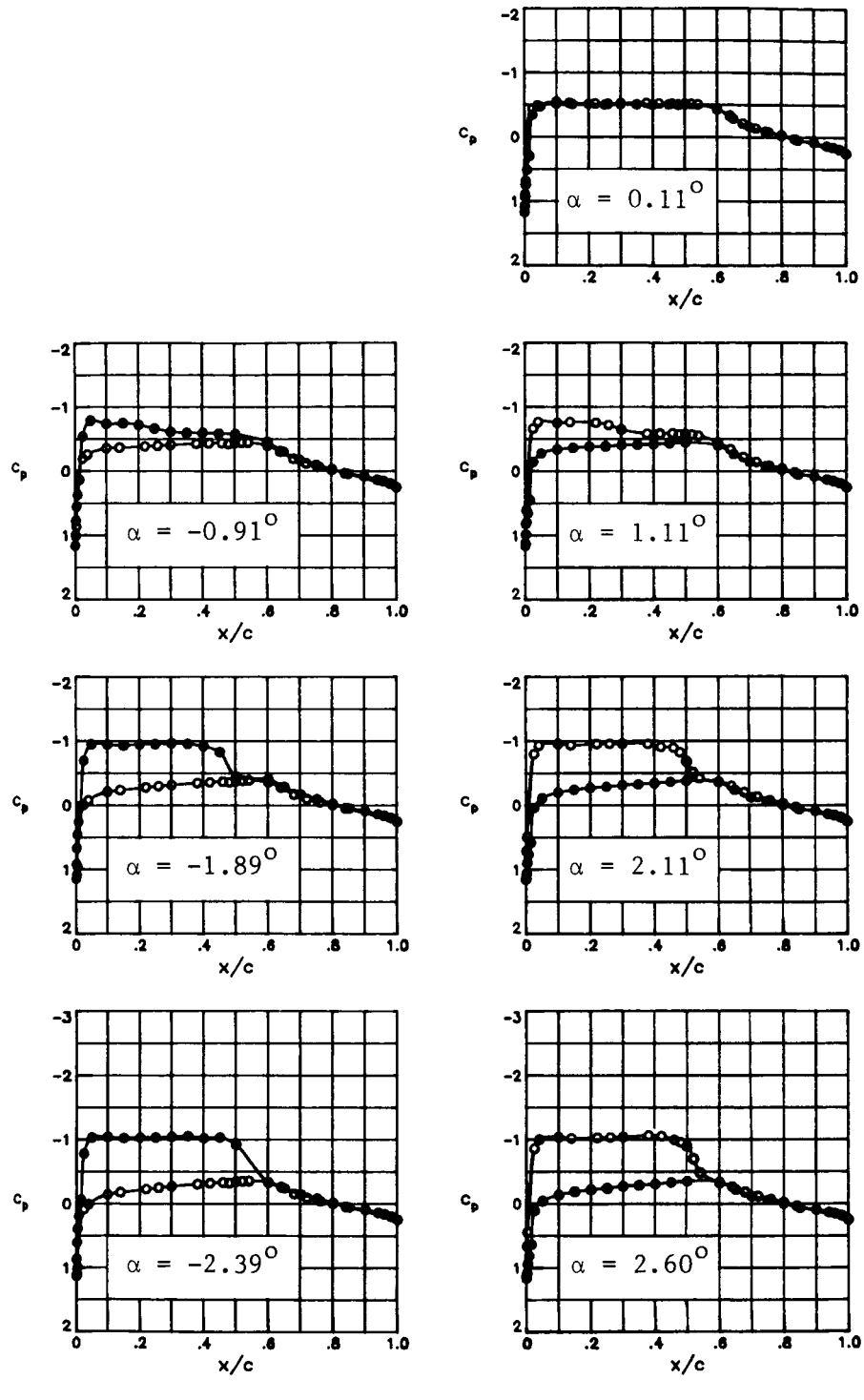

(d) $M_\infty = 0.78$.

Figure 15.- Continued.

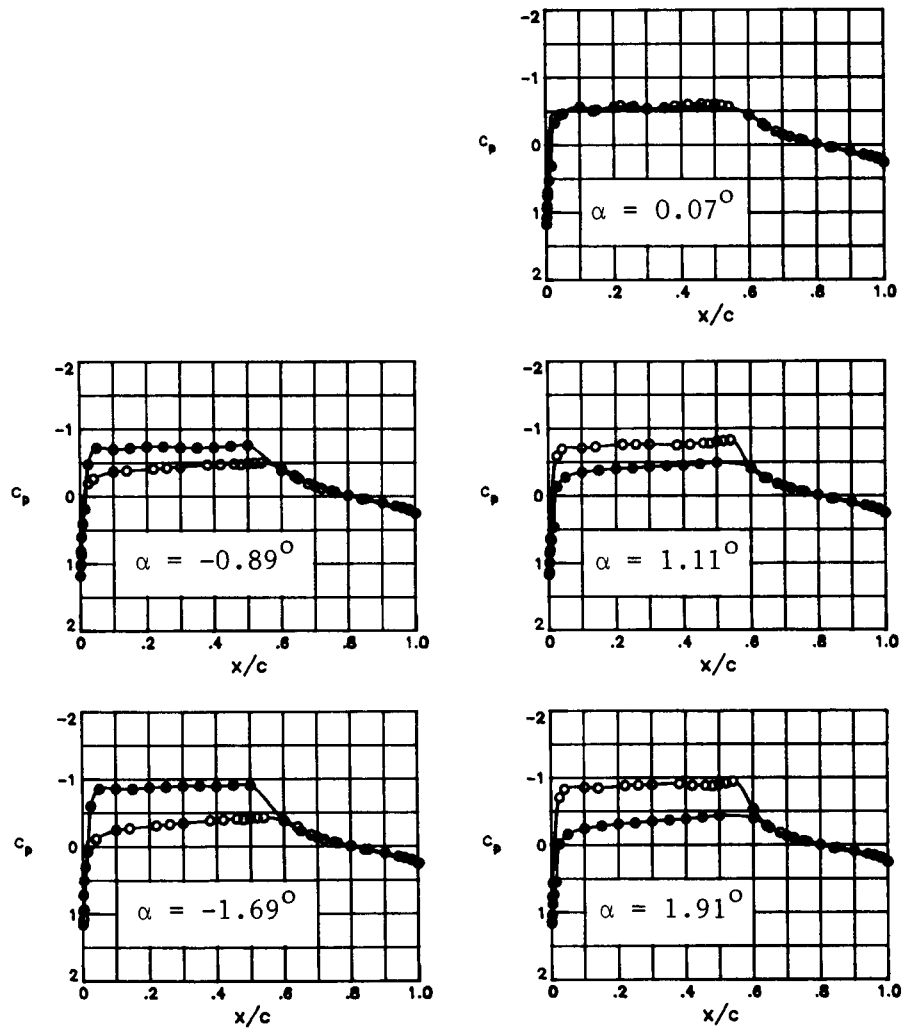

(e) $M_\infty = 0.80$.

Figure 15.- Concluded.

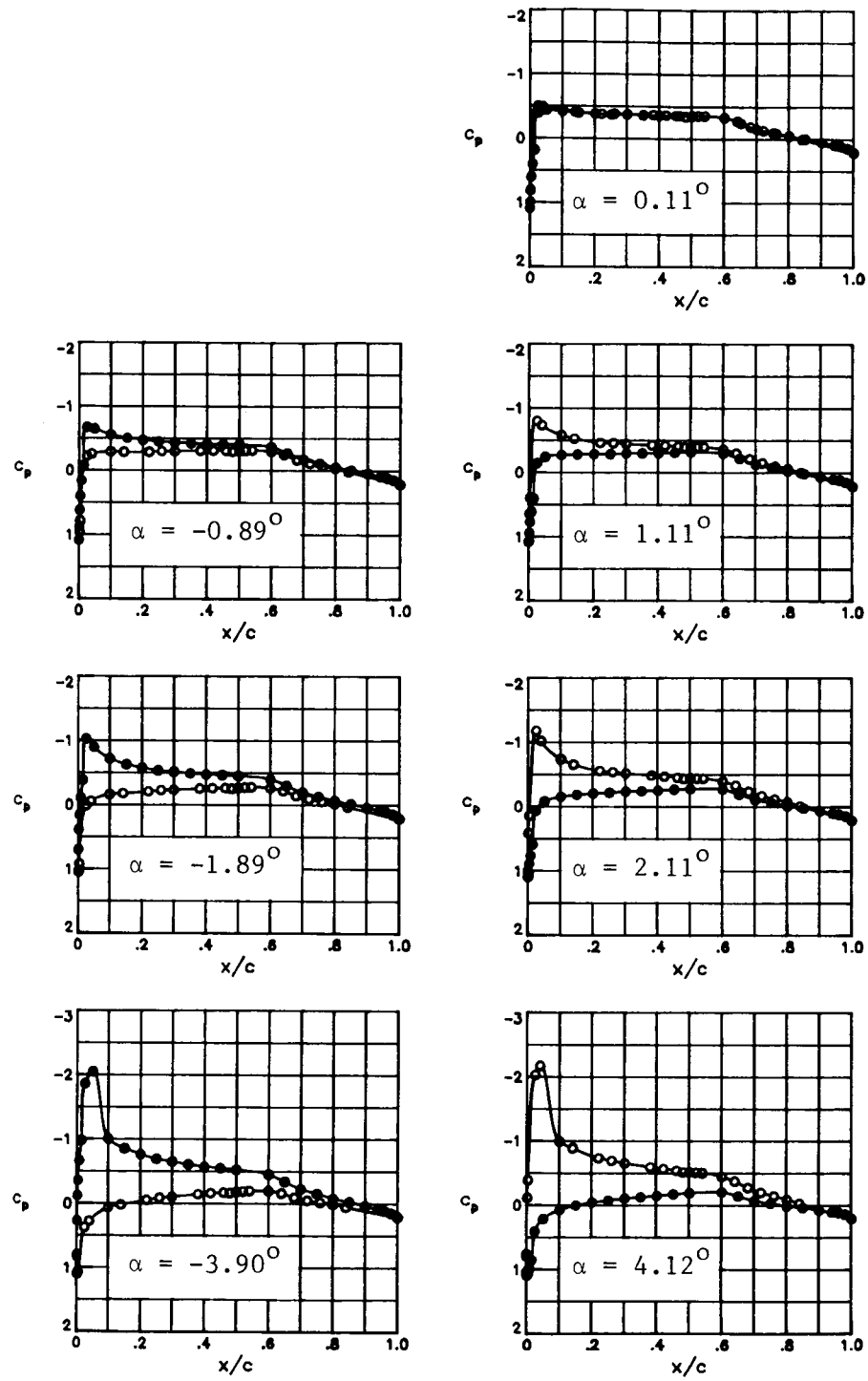

(a) $M_\infty = 0.60$.

Figure 16.- Effect of angle of attack on chordwise pressure distribution at $R_c = 40 \times 10^6$. Open symbols denote upper surface; solid symbols denote lower surface.

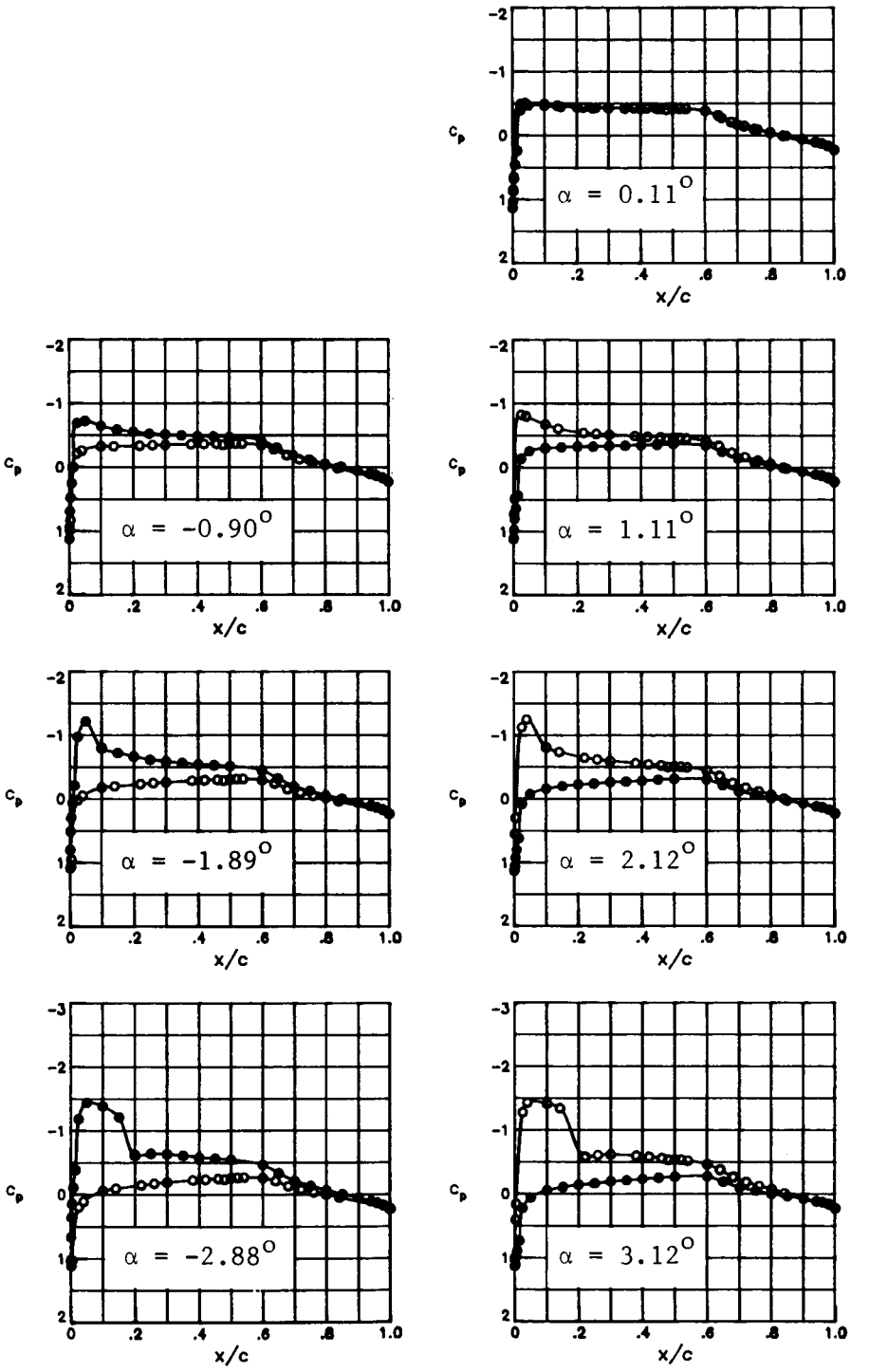

(b) $M_\infty = 0.70$.

Figure 16.- Continued.

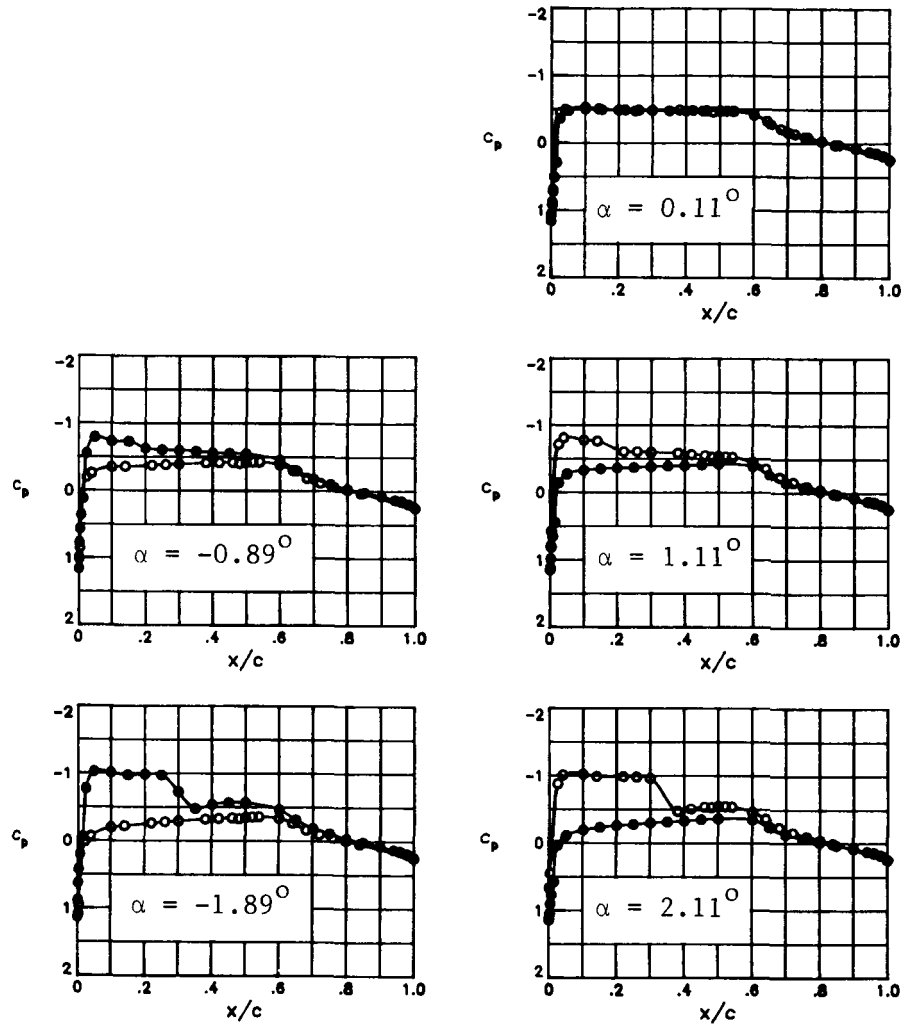

(c) $M_\infty = 0.77$.

Figure 16.- Continued.

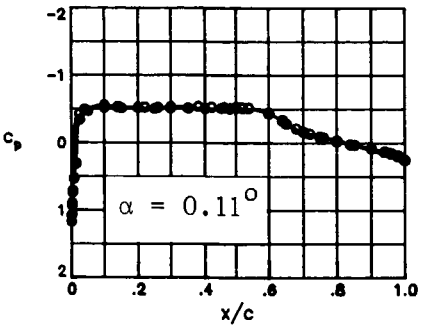

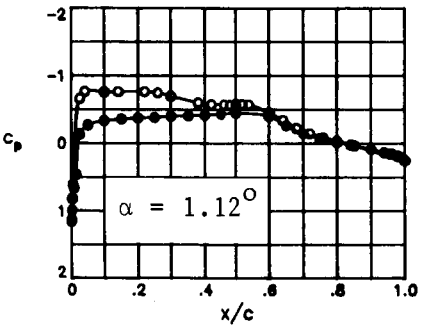

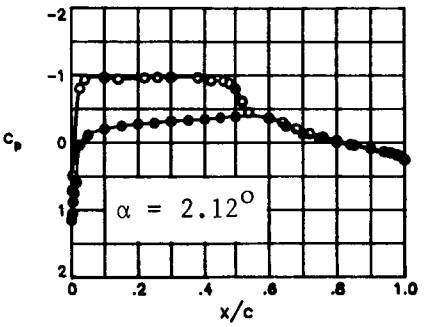

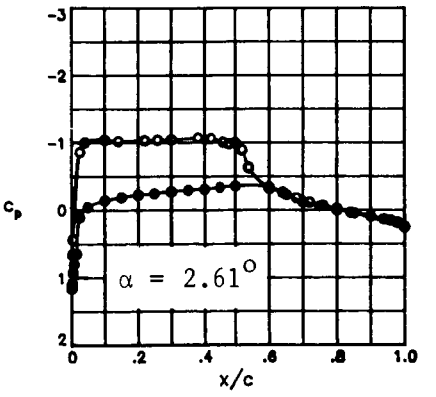

(d) $M_\infty = 0.78$.

Figure 16.- Continued.

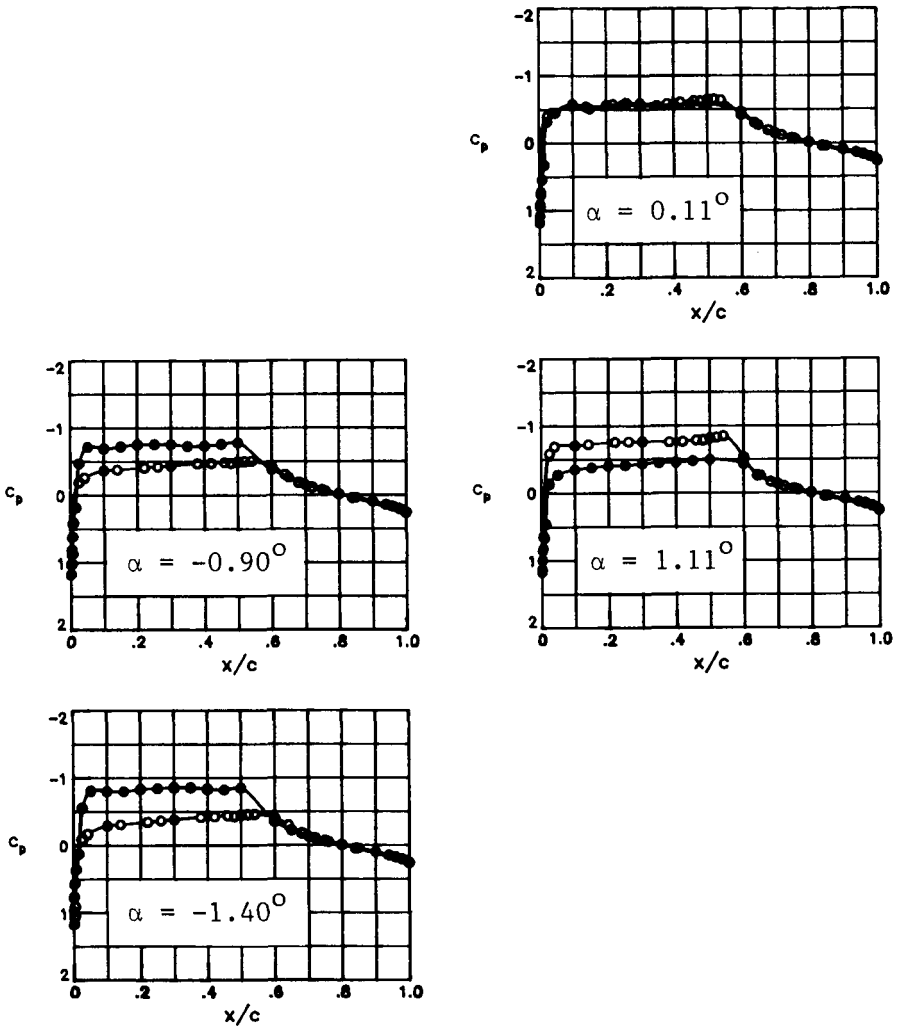

(e) $M_\infty = 0.80$.

Figure 16.- Concluded.

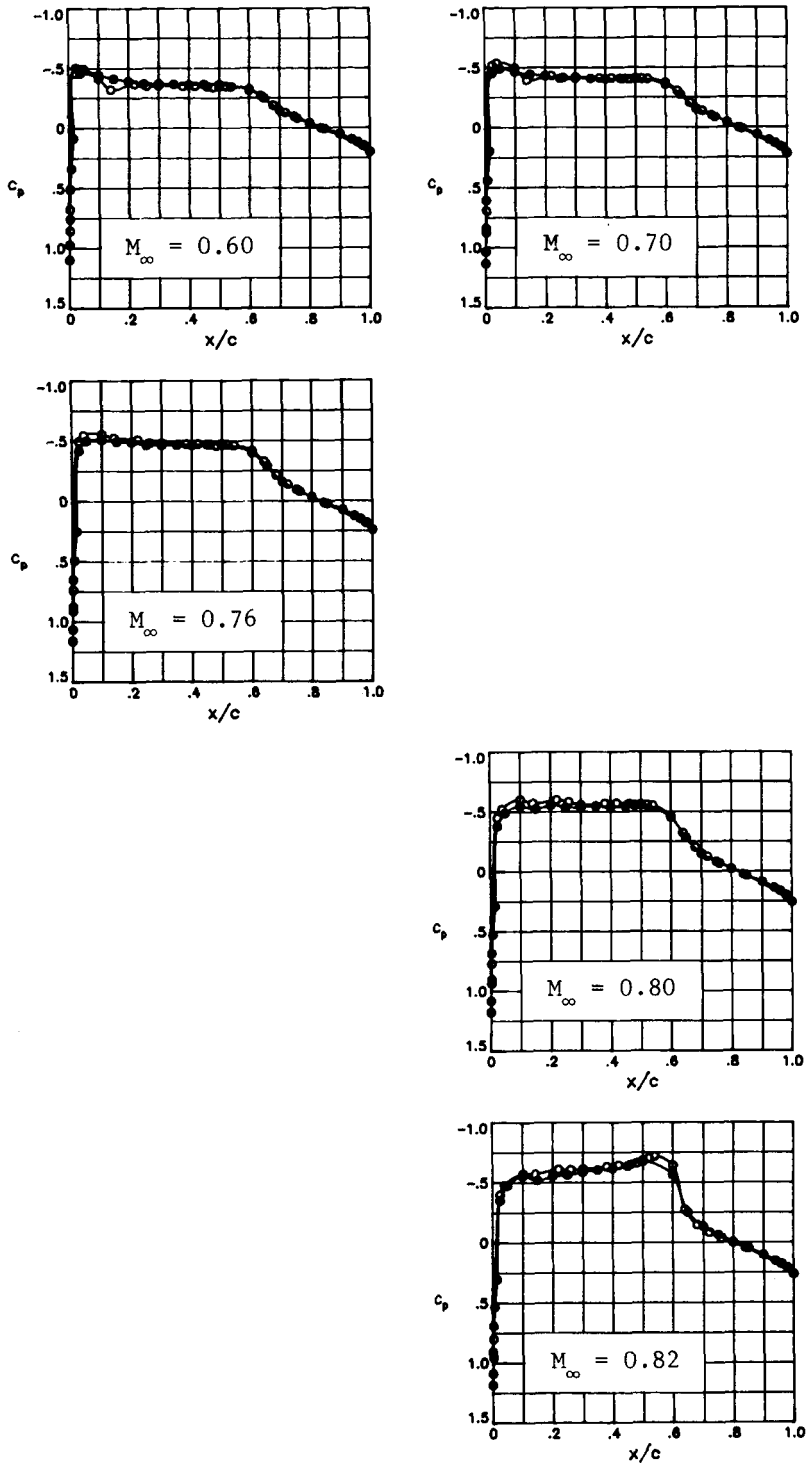

(a) $R_C = 6 \times 10^6$.

Figure 17.- Effect of Mach number on chordwise pressure distribution at $C_n \approx 0$. Open symbols denote upper surface; solid symbols denote lower surface.

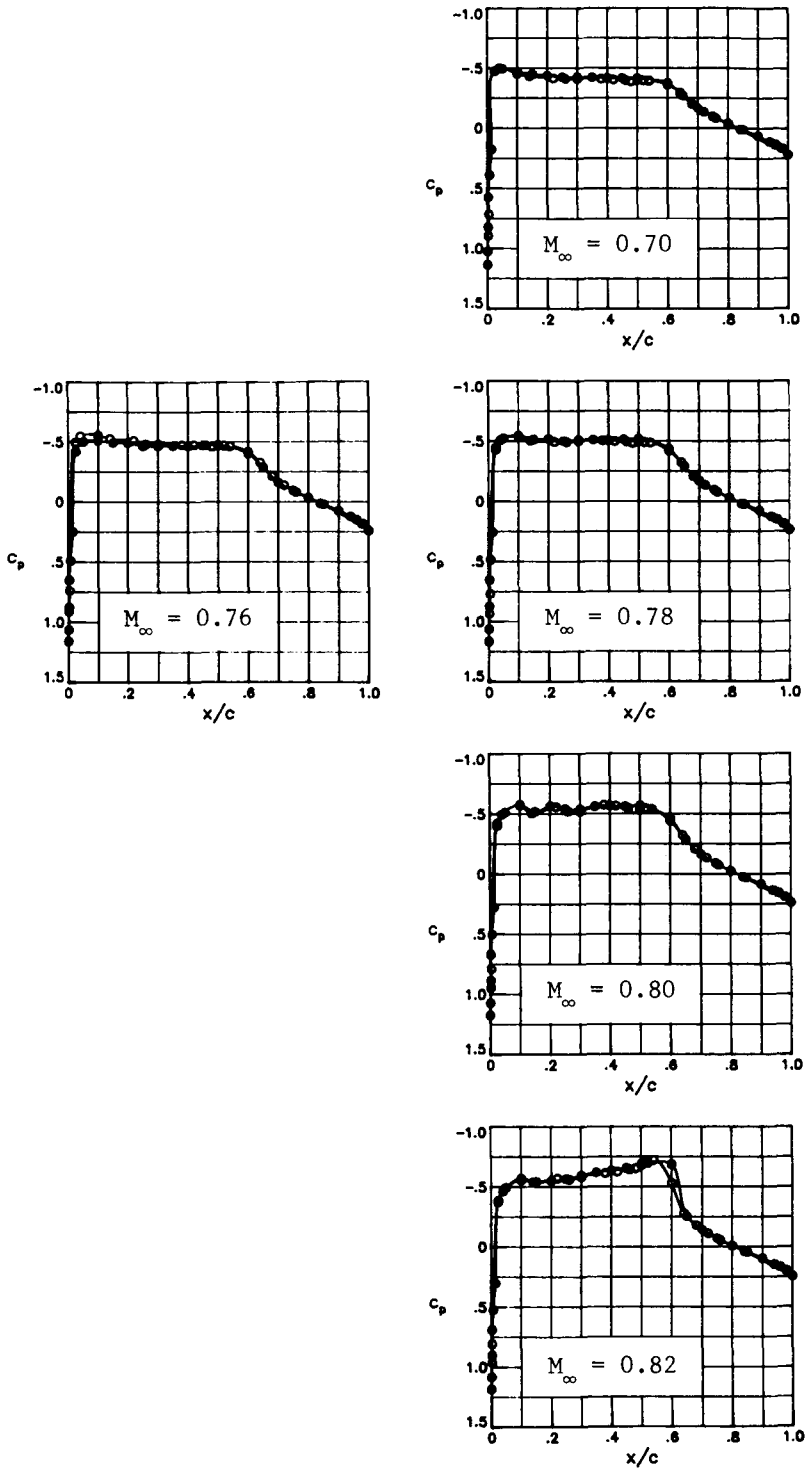

(b) $R_C = 9 \times 10^6$.

Figure 17.- Continued.

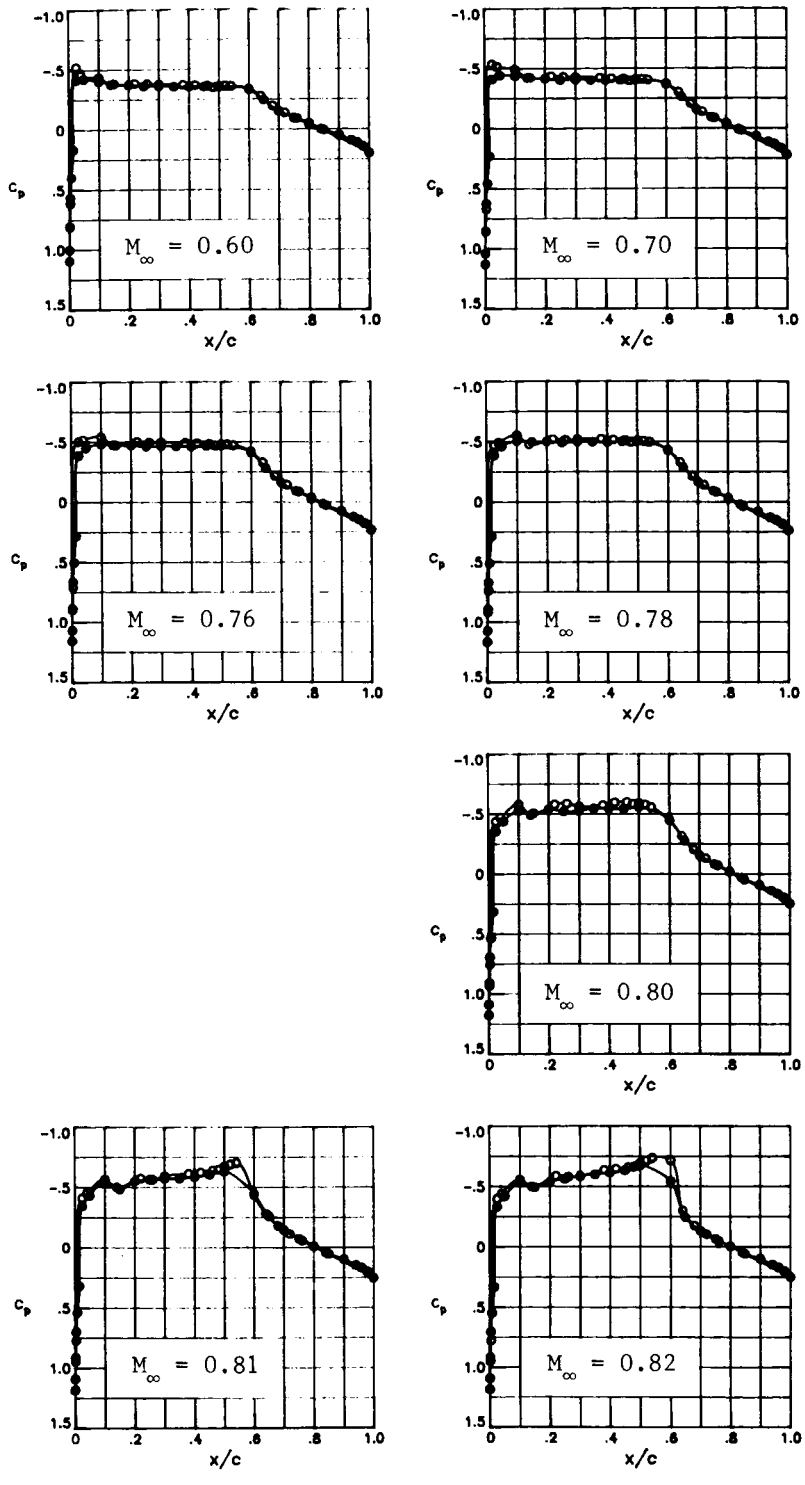

(c) $R_C = 15 \times 10^6$.

Figure 17.- Continued.

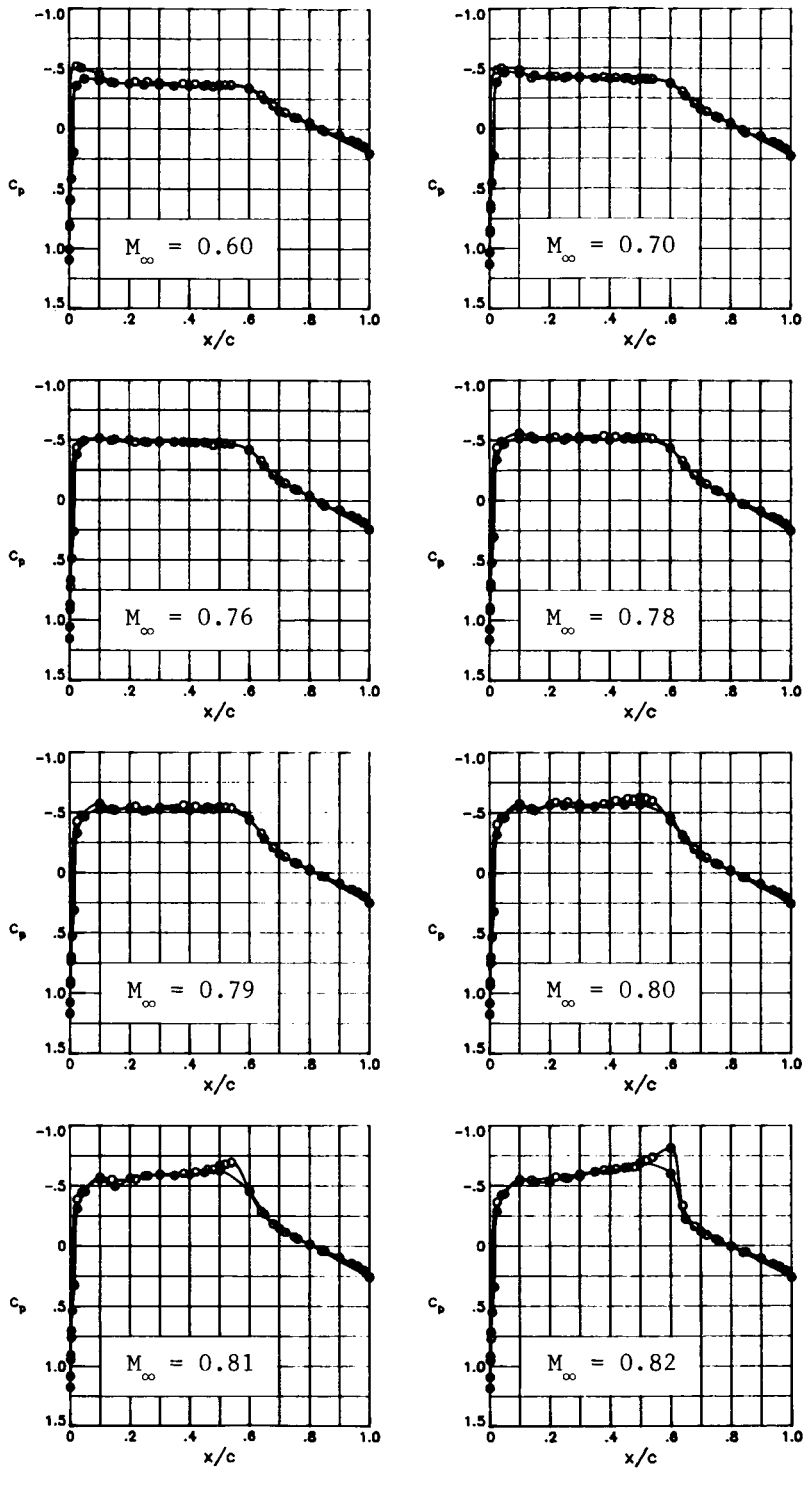

(d) $R_c = 30 \times 10^6$.

Figure 17.- Continued.

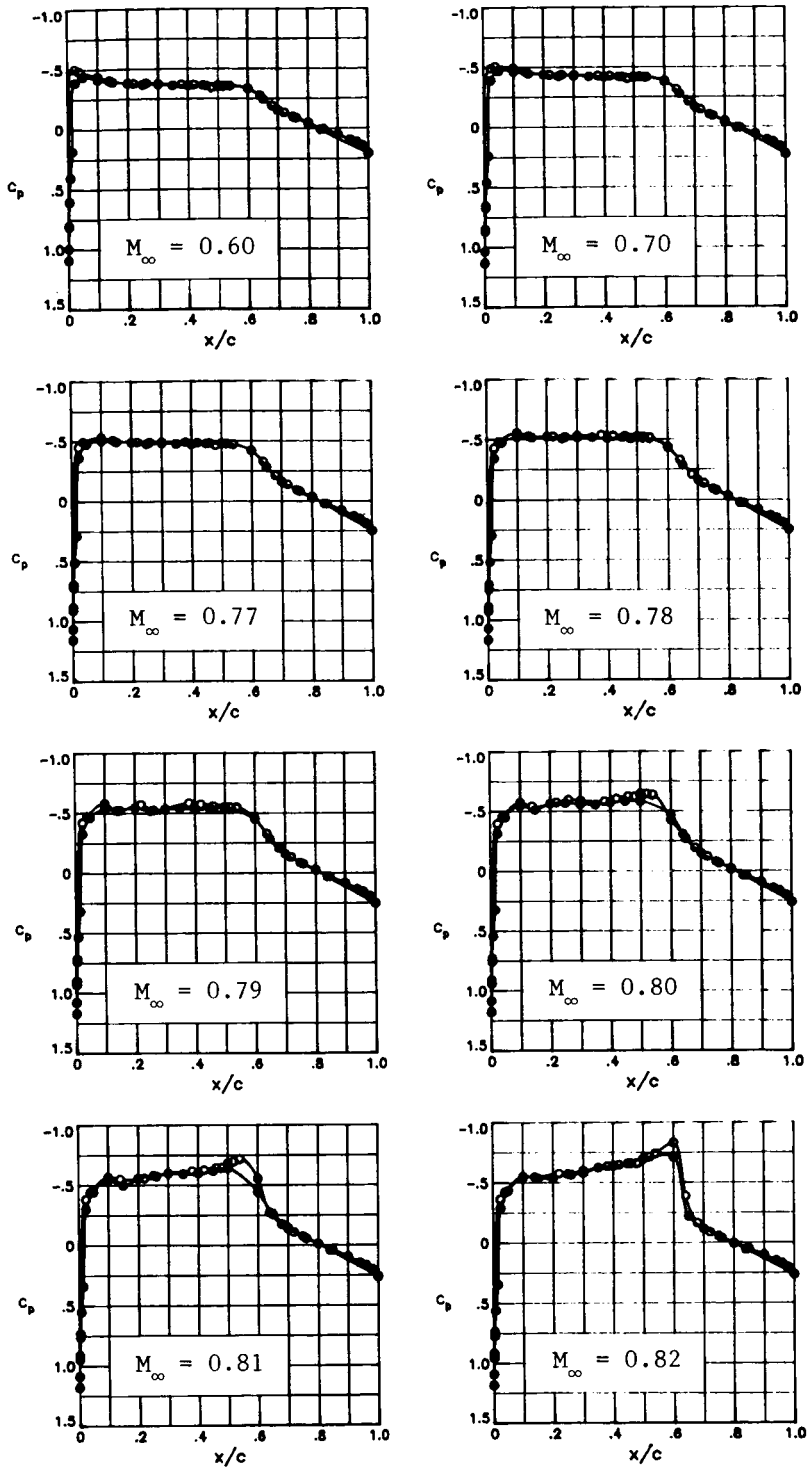

(e) $R_C = 40 \times 10^6$.

Figure 17.- Concluded.

Standard Bibliographic Page

1. Report No.	2. Government Accession No.	3. Recipient's Catalog No.
NASA TM-89102		

4. Title and Subtitle	5. Report Date
High Reynolds Number Tests of the NASA SC(2)-0012 Airfoil in the Langley 0.3-Meter Transonic Cryogenic Tunnel	July 1987
	6. Performing Organization Code
7. Author(s)	8. Performing Organization Report No.
Raymond E. Mineck and Pierce L. Lawing	L-16259
9. Performing Organization Name and Address	10. Work Unit No.
NASA Langley Research Center Hampton, VA 23665-5225	505-61-01-02
	11. Contract or Grant No.
12. Sponsoring Agency Name and Address	13. Type of Report and Period Covered
National Aeronautics and Space Administration Washington, DC 20546-0001	Technical Memorandum
	14. Sponsoring Agency Code

15. Supplementary Notes

16. Abstract

A wind-tunnel investigation of the NASA SC(2)-0012 airfoil has been conducted in the Langley 0.3-Meter Transonic Cryogenic Tunnel. This investigation supplements the two-dimensional airfoil studies of the Advanced Technology Airfoil Test program. The Mach number was varied from 0.60 to 0.84. The stagnation temperature and pressure were varied to provide a Reynolds number range from 6 to 40 $\times$ 10^6 based on a 6.0-in. (15.24-cm) airfoil chord. No corrections for wind-tunnel wall interference have been made to the data. The aerodynamic results are presented as integrated force and moment coefficients and pressure distributions without any analysis.

17. Key Words (Suggested by Authors(s))	18. Distribution Statement
High Reynolds number Symmetric airfoil Supercritical airfoil	Unclassified - Unlimited Subject Category 02

19. Security Classif.(of this report)	20. Security Classif.(of this page)	21. No. of Pages	22. Price
Unclassified	Unclassified	56	A04

For sale by the National Technical Information Service, Springfield, Virginia 22161